González-García, Estefanía et al., 2020. Nanomaterials in Protein Sample Preparation. Separation and Purification Reviews, 49(3), pp.229-264.

NANOMATERIALS IN PROTEIN SAMPLE PREPARATION

Estefanía González-García, María Luisa Marina, María Concepción García *

Departamento de Química Analítica, Química Física e Ingeniería Química, Instituto de Investigación Química "Andrés M. del Río" (IQAR), Universidad de Alcalá, Ctra. Madrid-Barcelona km 33.600, 28871, Alcalá de Henares (Madrid), Spain

* Corresponding author: concepcion.garcia@uah.es

ABSTRACT

Protein sample preparation is the most critical step in protein analysis of complex samples and is constituted by tedious, time-consuming and difficult to automate steps that usually involve the use of high solvents volumes. In recent years, novel nanomaterials have been developed aiming to overcome these drawbacks. In this review, we have grouped those works related to the development of new nanomaterials and their applications to the extraction, enrichment/purification, and digestion of proteins. This paper evaluates the role of different kinds of nanomaterials in each step of protein sample preparation focusing on the type of established interaction between the protein and the nanomaterial, their sensitivity and selectivity, their adsorption capacity, and the advantages that they suppose in relation to time, efficiency, or reusability.

Keywords: Protein sample preparation, nanomaterials, extraction, enrichment, purification, digestion, enzyme.

ACRONYMS

AgNPs	Silver nanoparticles
ANTA	Nα,Nα-Bis(carboxymethyl)-L-lysine hydrate
APTES	3-Aminopropyltriethoxysilane
ARPCs	Assistant recognition polymer chains
AuNPs	Gold nanoparticles
BFg	Bovine fibrinogen
BSA	Bovine serum albumin
CNTs	Carbon nanotubes
CTA	Cetyltrimethylammonium

Cyto C	Cytochrome C
DESs	Deep eutectic solvents
DIH	1, 6-Diisocyanatohexan
dsRNA	double-stranded RNA
EDTA	ethylene diamine tetraacetic acid
EMIMLpro	1-Ethyl-3-methyl-imidazolium L-proline
GMA	Glycidyl methacrylate
GMA-co-EDMA	Glycidyl methacrylate-co-ethylene dimethacrylate
GO	Graphene oxide
His-tag	Histidine-tagged
IDA	Iminodiacetic acid
ILs	Ionic liquids
MALDI(-MS)	Matrix-assisted laser desorption/ionization(-mass spectrometry)
MBISA	2-Mercapto-5-benzimidazolesulfonic acid
ME-MIONs	Microemulsion magnetic iron oxide nanoparticles
MIP	Molecularly imprinted polymer
MNPs	Magnetic nanoparticles
MS	Mass spectrometry
MWCNTs	Multi-walled carbon nanotubes
NAaP	Nucleic acid associated proteins
NMs	Nanomaterials
NPs	Nanoparticles
oMWCNT	oxidized multiwall carbon nanotubes
PDDA	poly(diallyldimethylammonium chloride)
PDMS	Polydimethylsiloxane
PEG	Polyethylen glycol
PEI	Polyethyleneimine
PHEMATrp	Poly(hydroxyethyl methacrylate-N-methacryloyl-(L)-tryptophan)
SDS-PAGE	Sodium dodecyl sulfate-polyacrylamide gel electrophoresis
SWCNTs	Single-walled carbon nanotubes
TOF	Time of flight

19

INTRODUCTION

The most critical step to obtain reliable results when analyzing proteins is a correct protein sample preparation. It mainly involves the extraction of proteins, the enrichment/purification of proteins, and, in some cases, also the digestion of proteins.

Protein extraction is a process that enables the separation of proteins from the rest of sample and that requires the breakdown of tissues with the aim to release the intracellular material. Protein extraction, purification, and enrichment, in the case of plant tissues, is limited by the plant structural complexity and rigid cell walls, the presence of high amounts of non-protein compounds (e.g. phenolic compounds or lipids) and the large dynamic protein concentration range [1,2]. In the case of animal tissues, tissues disrupting methods are required to break impermeable barriers and to overcome mass transfer obstacle [3].

There are several conventional methods enabling protein extraction, purification, and enrichment. Protein extraction is usually based on the utilization of surfactants as sodium dodecyl sulfate (SDS), Triton X, and Tween [4] or organic solvents as acetone, toluene, and chloroform [5]. In some cases, extraction buffer contains additives such as ethylene diamine tetraacetic acid (EDTA), dithiothreitol, or 2-mercaptoethanol, which enable protein denaturation and disruption of disulfide bonds [4]. In general, and especially when surfactants are employed, a purification step is required to remove surfactants and secondary metabolites that are coextracted with proteins and that can interfere in separation and analysis of proteins. Additionally, protein enrichment is required when extracted proteins are in low concentration. There are numerous strategies allowing the removal of interfering compounds and that can be carried out before or after the extraction of proteins. Among the methods that are applied previously to the extraction of proteins are those based on the use of trichloroacetic acid (TCA)/acetone, phenol, or TCA/acetone/phenol. These methods are highly effective for complex samples, but they are long, tedious, and require high solvents volumes, which make them non-sustainable [1]. Among the purification methods, applied after protein extraction, are the precipitation of proteins by adding organic solvents, acids, salts, or polymers or by changing temperature or pH. These methods also enable the enrichment

of proteins. The addition of acetone [6] or TCA [7] produces the protein precipitation based on their denaturation under hydrophobic or acidic conditions. These methods can be employed to remove surfactants, but they are not as effective as the use of TCA/acetone, phenol, or TCA/acetone/phenol and they are not suitable to extract native proteins. Another approach is the use of the chloroform-methanol-water system [8], where proteins precipitate in the interphase between methanol and water (upper layer) and chloroform (lower layer). After removing the upper layer, methanol is added to the chloroform to reduce its density and proteins are recovered by centrifuging the solution. This method is indicated for both soluble and hydrophobic proteins and is effective in the removal of interfering compounds, but it requires the use of toxic solvents. Thermal, isoelectric point, and "salting out" precipitation are fast and cheap methods. The increase of the temperature or the variation of the pH results in the precipitation of proteins [4,9], but these strategies do not guarantee the precipitation of all proteins. The saturation of the solution with salts also produce the precipitation of proteins, but it requires the use of a desalting step by dialysis [4,10]. Polymers can be also applied to precipitate proteins. The neutral polymer polyethylene glycol (PEG) [11], triggers the precipitation of proteins based on a volume exclusion effect. This method is fast and do not produce the denaturation of proteins, but it requires a high quantity of polymer. On the other hand, the cationic polymer polyethyleneimine (PEI) induces the coprecipitation of acidic proteins when it is in saline conditions, but it requires a removal step [12]. Another strategy is the ultrafiltration through molecular weight cut-off filters [4], that enables the separation of proteins from interfering compounds with different molecular masses. However, expensive ultrafiltration filters can become easily blocked. Moreover, chromatographic (e.g. ion exchange or hydrophobic interaction chromatography) or electrophoretic techniques (e.g. isoelectric focusing) [10] are widely used for protein purification. Nevertheless, they require long-time separations and, in the case of chromatography, high solvent volumes. Finally, protein digestion could also be a critical step, due to the long incubation times (overnight) usually needed, to its difficult automatization, and to a high enzyme consumption [13].

The emergence of new nanomaterials (NMs) have open new opportunities to face the extraction, purification/enrichment, and digestion of proteins. NMs are materials with, at least, one of their dimensions in the nanoscale (1-100 nm). Due to their dimensions, they show different characteristics from their corresponding bulk material [14,15]. NMs present extraordinary mechanical properties, mainly due to the short bond length between their atoms [15] and to their lower structure imperfections [16]. Additionally, they possess enhanced electrical, magnetic, optical, thermal, and chemical properties in comparison to their corresponding bulk materials. Moreover, they show good reactivity and can be easily functionalized [15,16]. This higher reactivity can be attributed to changes in the surface free energy and the electronic structure, and to variations in the atomic structure due to their reduced size [17].

NMs can present different morphologies depending on the number of dimensions that are not in the nanoscale. Thereby, NMs can be classified into 0-, 1-, 2-, and 3-dimension NMs (0-D, 1-D, 2-D, and 3-D NMs, respectively). NMs with all their dimensions in the nanoscale are called 0-D as, for example, nanoparticles (NPs), quantum dots, and fullerenes. 1-D NMs are those with two dimensions in the nanoscale, such as nanotubes, nanowires, and nanorods. NMs with just one nanosized dimension are called 2-D NMs and show sheet shape, such as graphene and graphene oxide (GO). Finally, 3-D NMs are nanostructured materials, as the case of nanoporous metals or zeolites [15,18]. Regarding their chemical composition, NMs can be classified into four main groups: carbon-based materials, metal-based materials, dendrimers, and composites [17,19].

Carbon-based materials, as their name implies, have carbon as main component. Depending on the shape they adopt, they receive different names. Thus, carbon-based materials with spherical or sheet shape are fullerene and graphene, respectively, while carbon-based NMs with tube shape are single- or multi-walled carbon nanotubes (SWCNTs or MWCNTs, respectively) [17,19]. Regarding their applications, fullerenes have been employed in the development of fuels and solar cells [20-22], in dermatological and cosmetic applications [23], and, also, in biological and pharmaceutical fields [24]. Graphene has been mainly used in fluorescence and electrochemical (bio)sensing [25,26], but also, for preparing microbial fuel cells

100 [27] or as antibacterial [28]. Carbon nanotubes also have many applications, such as pesticides
101 extraction [29], nanocarriers and biomedical applications [30], disease diagnosis, cellular
102 imaging, and drug targeted delivery [31].

103 On the other hand, metal-based materials can refer to metal oxides (e.g. TiO_2 or ZnO),
104 noble metal NMs (e.g. Au, Ag, or Fe) or QDs (e.g. ZnSe or CdSe), which are semiconductor
105 crystal nanostructures made of hundreds of thousands of atoms and with a variable size [17,19].
106 Regarding their application, several metal oxide NPs have been used as antimicrobial agents or
107 in drug delivery applications [32,33]. ZnO has been widely employed in sensing, imaging, drug
108 delivery, and for food applications [34,35]. Noble metal NPs as gold NPs (AuNPs) and silver NPs
109 (AgNPs) have been used in cancer diagnosis and treatment, imaging, food industry, biosensing,
110 or catalysis among others [36], similarly to Fe-containing NPs [37]. Another example of metal-
111 based materials is CdSe QDs, which have been employed in electronic devices, bioanalysis, or
112 imaging [38].

113 Dendrimers, the third big group of NMs, are a kind of 3-D NM with an hyperbranched
114 structure. Their properties can be easily tuned and their terminal branches can be tailored with
115 functional groups. The presence of cavities in their structure makes them potential host molecules
116 [17,19]. Polyamidoamine (PAMAM) and polypropylene imine (PPI) are the most known and used
117 dendrimers, being also commercially available [39]. Furthermore, carbosilane dendrimers have
118 emerged as a new kind of dendrimers with extraordinary properties and potential for several
119 applications [40]. Dendrimers have been used for disease diagnosis and treatment, drug delivery
120 agents, catalysis, and cosmetics [39,41].

121 Finally, composites are made with two or more interacting materials, for example NMs in
122 combination with a bulk material. Materials can be combined by filling, mixing or assembling
123 [17,42]. It is common to use the symbol "@" to refer to "coating" when naming the composites.
124 For example, X@Y means that Y is coating X. Most popular composites are graphene-based,
125 which have been widely employed in sensing [26]. Moreover, GO composites have been used in
126 photocatalytic and antibacterial applications [43], while carbon nanotubes (CNTs)-metal oxide

nanocomposites were profitable to build supercapacitors, in photocatalysis, or in sensing applications [44].

Many applications of NMs are based on their interaction with proteins [45]. Moreover, the strong interaction between proteins and many NMs have been exploited in the extraction, digestion, and purification/enrichment of proteins. Part of these applications have appeared in revisions devoted to very specific issues (liquid-phase microextraction, sugar immobilized AuNPs, MNPs, etc.) and not entirely focused on proteins [46-53] (see **Table 1**). Thus, the present work arises with the aim to review the works devoted to the development and application of NMs to the extraction, enrichment/purification, and digestion of exclusively proteins. Moreover, different commercial NPs for the extraction and purification of proteins are named.

EXTRACTION OF PROTEINS FROM COMPLEX SAMPLES USING NANOMATERIALS

Protein extraction is the process that enables the separation of proteins from the rest of components of a complex matrix, which can contain polyphenols, polysaccharides, lipids, or others not desired compounds. It is the first step in protein sample preparation. The development of new strategies based on NMs is an increasing trend to overcome the limitations presented by conventional extraction methods (time-consuming, high solvent volumes, etc.). **Table 2** groups the works that use NMs for the extraction of proteins from complex samples.

Carbon-based NMs

Carbon nanotubes have been employed for the extraction of proteins based either on chelation through metal cations or on electrostatic interactions. In 2006, Najam-ul-Haq et al. [54] synthesized a new material for protein extraction that was employed for the profiling of proteins through material-enhanced laser desorption/ionization-mass spectrometry. This material consisted of CNTs modified with iminodiacetic acid (IDA) and loaded with Cu^{2+}. This material permitted the extraction of proteins by chelation within 90 min and the direct analysis of minor

153 proteins in human serum without the previous depletion of high abundant serum proteins,
154 obtaining high sensitivity and selectivity. Lately, in 2013, Du et al. [55] employed another carbon-
155 based nanomaterial (polyethyleneimine modified MWCNTs (MWCNTs–PEI) adsorbed on a
156 membrane) but, in this case, the interactions with proteins were not through a metal cation, as
157 previously, but directly with the material through electrostatic forces. They applied it to the
158 extraction of bovine serum albumin (BSA) from a bovine serum sample. Main advantage of this
159 material was the low limit of detection (LOD = 1.0 μg/mL) and the high BSA adsorption capacity
160 (113 mg/g MWCNTs) derived from the high density of functional groups provided by PEI.
161 Moreover, authors demonstrated that this membrane could be used, for at least, 60 times without
162 losing capacity.

163 Magnetic metal-based NMs

164 Iron NPs are of great interest since their magnetic properties make faster and easier the
165 separation of proteins from non-interacting compounds. **Figure 1** shows the scheme of a typical
166 extraction employing magnetic nanoparticles (MNPs). Briefly, it consists of adding the MNPs,
167 incubation until the interaction is produced, magnetic separation of captured proteins,
168 nanoparticles wash to remove unbound compounds, elution of proteins, and recovery of MNPs
169 for next uses. Shukoor et al. [56] took advantage of the magnetic properties of superparamagnetic
170 γ-Fe_2O_3 NPs coated with a polymer to selectively extract a 35 kDa protein from a demosponge,
171 based on its specific bind to the double-stranded RNA. Iron MNPs modified with ionic liquids
172 (IL) have also been used in the extraction of proteins [51, 52]. ILs are a type of organic salts with
173 extraordinary physical and chemical properties that have a great potential as solvent and
174 functional materials. Moreover, amino acid-based ILs are biocompatible and can establish
175 multiple interactions with proteins. Wang's group [57] developed a magnetic solid-phase
176 extraction cartridge based on Fe_3O_4 NPs where a L-proline-based ionic liquid (IL) (1-ethyl-3-
177 methylimidazolium L-proline, EMIMLpro) was introduced by 6-diisocyanatohexane (DIH). The
178 developed magnetic sorbent, Fe_3O_4@DIH-EMIMLpro, extracted hemoglobin from a human
179 blood sample through adsorption and electrostatic forces within just 15 min. Moreover, authors

evaluated the binding specificity of these NPs by extracting hemoglobin from a mixture containing lysozyme. Results demonstrated the negligible adsorption of lysozyme even presenting the double concentration than hemoglobin. On the other hand, Liu et al. [58] employed another ionic liquid, *N*-methylimidazolium, attached to a silica coated MNP (Fe_3O_4@SiO_2@ILs) to extract hemoglobin from human blood but, in this case, through complexation forces. In this work, authors demonstrated the binding selectivity of these NPs in different binary protein mixtures. Both NMs [51, 52] were reusable but Fe_3O_4@SiO_2@ILs showed a binding capacity 4 times higher than Fe_3O_4@DIH-EMIMLpro.

Molecularly imprinted polymers (MIPs) have been widely used for the selective extraction of a plethora of compounds, including proteins [59]. MIPs have also been combined with NMs and applied to the extraction of proteins. A thermoresponsive material based on a MIP enabled the capture of lysozyme from human urine in 2 h [60]. This material consisted of a magnetic core/shell structure of Fe_3O_4@SiO_2 coated with γ-methacryloxypropyltrimethoxysilane and polymerized in presence of lysozyme. To test the specificity of this material, authors also synthesized not-imprinted NPs. In first instance, they tested the behavior of these two NPs when changing the temperature, observing the decrease of hydrodynamic size of NPs when increasing the temperature. They also demonstrated that the capacity to adsorb lysozyme was related to the swell/shrink behavior of NPs. At all tested temperatures, imprinted NPs presented higher lysozyme adsorption capacity than non-imprinted ones. Moreover, non-imprinted NPs showed non-specific adsorption, especially at high temperatures (40 ºC). The binding selectivity of imprinted NPs was tested by employing different proteins that yielded a very low adsorption capacity compared to lysozyme. In the case of pepsin and BSA, the low adsorption capacity was related to their higher size and, thus, to a steric impediment. In the case of Cyto C, the low adsorption was attributed to the difference in hydrophobicity with respect to lysozyme. Finally, in the case of myoglobin, the low adsorption was related to the lack of electrostatic interactions when capturing this uncharged protein. According to these results, the specific interaction between lysozyme and MIP-based NPs was driven by the size, hydrophobicity, and charge. As

example, **Figure 2** shows the chromatograms obtained with two mixtures of lysozyme and Cyto C when no treating with Fe_3O_4@MIP NPs (1) and after treating with Fe_3O_4@MIP NPs (3). Results demonstrated the high selectivity of these NPs, that were able to capture lysozyme even in presence of twice concentration of Cyto C.

Metal-based NMs have been widely used for the extraction and purification of recombinant histidine-tagged (His-tag) proteins. Genomics enables the easy introduction of histidine tags in proteins and express them in hosts, such as *Escherichia coli* (*E. coli*) or *Pichia pastoris* (*P. pastoris*). These tags can interact with affinity ions, e.g. Ni^{2+} [61,62]. Yao et al. [63] employed Fe_3O_4@hydroxyapatite-Ni^{2+} NPs for the extraction, in 2 h, of His-tag proteins from an *E. coli* cell lysate by means of affinity interactions observing a negligible nonspecific adsorption. Some benefits of these NPs are their easy, cost-effective and efficient synthesis and the high number of active sites provided for the hydroxyapatite for the Ni^{2+} binding.

Additionally, there are diverse commercial MNPs aimed to the affinity extraction and purification of proteins, such as, MagVigen™ from NVIGEN (diameters of 200-500 nm), μMACS™ and MultiMACS™ from Miltenyi Biotech (diameters of 50 nm), and TurboBeads™ from TurboBeads (also available from Sigma-Aldrich) (diameters of ≤ 30 nm). The main advantage of these NPs with respect to other commercial microbeads is their smaller size and, thus, their higher surface area for protein adsorption. Moreover, TurboBeads™, unlike the rest of MNPs, present a pure metallic core, that provided them an enhanced magnetism, and a coating with a graphene-like carbon layer of about 2 nm, that improve their functionalization feasibility. Commercial MNPs are available with a great variety of functionalities (Protein A and G, Streptavidin, Biotin, amine groups, hydroxyl groups, Ni^{2+}, among others) that offer a wide range of applications. In general, the extraction times when employing these NPs range from 10 min to 2 h, depending on the protein, and they are highly reusable.

Non-magnetic metal-based NMs

Non-magnetic metal-based NMs have also been applied in protein extraction processes. The extraction of hydrophobic proteins from soybean was carried out in 1 h employing different kinds of metal-based NMs: Ag_2Se@octadecanethiol and Ag_2Se@11-mercaptoundecanoic acid NPs [64]. These NMs were employed as extracting probes of proteins in liquid-phase microextraction for their analysis by matrix-assisted laser desorption/ionization-time of flight (MALDI-TOF) analysis. Moreover, they showed a high efficiency, even in presence of matrix interferences. Later, the same authors extracted hydrophobic proteins from bacteria *E. coli* and *Bacillus subtilis* (*B. subtilis*) using other non-magnetic metal-based NMs: $Mg(OH)_2$-oleic acid NPs [65] and $BaTiO_3$–12-hydroxy octadecanoic acid NPs [66]. Extraction of proteins was carried out in a lower time (45 and 30 min, respectively) than the previously needed (1 h). These materials enabled not just an efficient liquid-liquid microextraction, but also an excellent preconcentration prior to MALDI-TOF analysis.

Nanocomposites

Nanocomposites containing carbon-based materials, especially GO, have also been used in protein extraction. Bovine hemoglobin was extracted using a magnetic composite (Fe@GO) functionalized with an amino functional dicationic IL yielding a high adsorption capacity during, at least, 15 cycles and a low unspecific binding [67]. Additionally, different approaches were developed to extract BSA employing nanocomposites of Fe_3O_4 and GO. Xu et al. [68] functionalized a Fe_3O_4–NH_2@GO with different choline chloride (ChCl)-based deep eutectic solvents (DESs) finding that ChCl-glycerol was the most suitable for the extraction. DESs are eutectic mixtures of quaternary ammonium salts and hydrogen bond donors. DESs, like ILs, have unique physical and chemical properties, but, unlike them, DESs are biocompatible and biodegradable and they are not toxic. Huang et al. [69], on the other hand, grafted 3-aminopropyltriethoxysilane (APTES)-Fe_3O_4 NPs on the surface of GO and introduced a betaine-based IL. In the case of Fe_3O_4–NH_2@GO NPs [62], their functionalization with DESs resulted in higher extraction capacity than the obtained with Fe_3O_4–NH_2@GO and Fe_3O_4–NH_2. In the case of Fe_3O_4@APTES@GO@IL NPs [63], the same behavior was observed compared to

the individual components. In both cases, the NM-proteins interaction seemed to be related to the pH, ionic strength, temperature, extraction time, and protein and NM concentrations. Moreover, proteins eluting from these NMs maintained their structure. [68,69]. Nevertheless, platform using DESs (Fe_3O_4–NH_2@GO@ChCl-G) enabled shorter extraction times than the platform using ILs (Fe_3O_4@APTES@GO@IL), which resulted in a third of adsorption capacity.

Nanocomposites containing CNTs have also been employed for the extraction of different proteins. Tang et al. [70] applied coated polydimethylsiloxane (PDMS) fibers, as solid-phase microextraction materials, with SWCNTs and MWCNTs, for the extraction of BSA and bovine fibrinogen (BFg) from bovine plasma. Both PDMS@SWCNTs and PDMS@MWCNTs extracted these proteins through electrostatic interactions. SWCNTs had greater BSA adsorption capacity than MWCNTs due to their higher specific surface area. BFg showed a higher adsorptivity on MWCNTs than on SWCNTs that was attributed to the relative size of this big protein and the SWCNTs. Results also demonstrated the selectivity of the CNTs to the biggest protein (BFg) when its concentration reached a certain value and that the developed material presented higher selectivity and sensitivity than commercial PDMS fibers. Moreover, the extraction of BFg from bovine blood plasma was simple, time-saving, selective, and inexpensive. In other approach, oxidized MWCNTs (oMWCNTs), functionalized with magnetic Fe_3O_4 NPs, were employed to extract nucleic acid associated proteins (NAaP) [71]. oMWCNT@Fe_3O_4 enabled the capture of numerous NAaP, within just 1 min, based on the strong interaction established between CNTs and nucleic acids. This material enabled to capture 109 mg protein per g of nanocomposite and, also, the direct digestion of proteins for their MS analysis. Moreover, the specificity of this material was demonstrated by the SDS-PAGE analysis of a mixture of histone with BSA. Results showed negligible unspecific adsorption even when the concentration of BSA was ten times higher.

Quaresma et al. [72] synthesized star-shaped Fe_3O_4@AuNPs. These NPs maintained the original magnetic properties of the magnetite and, at the same time, they showed great optical properties and the possibility of biofunctionalization through the gold coating. In order to proof

286 the applicability of these NPs, they were functionalized with NTA-Ni^{2+} to selectively extract His-
287 tag proteins. The high selectivity of this material to His-tag proteins was demonstrated through
288 SDS-PAGE analysis.

289 Others

290 Other NM, poly(propargyl acrylate) NPs, that cannot be included in the four previous
291 groups, was used to extract carbazole 1-9a dioxygenase proteins from a *Pseudomonas*
292 *resinovorans* CA10 lysate in 1 h [73]. These poly(propargyl acrylate) NPs had attached an azide-
293 modified carbazole that is characterized by having an special affinity for these proteins, making
294 the process highly selective.

295

296 **PROTEIN ENRICHMENT/PURIFICATION USING NANOMATERIALS**

297 Protein extraction methods are usually not selective and an additional step for the
298 purification of proteins is sometimes needed. In other occasions, targeted proteins are in low
299 concentration limiting the application or identification of proteins. In these cases, protein
300 enrichment/purification methods are required to succeed in the research.

301 **Protein enrichment/(pre)concentration using nanomaterials**

302 This section groups those works devoted to the enrichment of proteins employing NMs
303 (see **Table 3**). Since many works using NMs for protein extraction (**Table 2**) also enrich or purify
304 them, they have not been included in **Table 3** for already being in **Table 2**. Thus, Table 3 groups
305 those works where proteins have been enriched after their extraction employing methods that did
306 not involve the use of NMs and resulted in low protein/s concentrations.

307 Carbon-based NMs

308 MWCNTs have demonstrated a great potential in the enrichment/(pre)concentration of
309 proteins [74-77]. Electrostatic interactions play an important role in this process. Both bare
310 MWCNTs [68, 69] and SiO_2@MWCNTs [76] were used for the enrichment of proteins. A higher

311 enrichment factor was obtained with MWCNTs-coated silica than with free MWCNTs.
312 Poly(diallyldimethylammonium chloride) (PDDA) have also been used to functionalize
313 MWCNTs [77]. This system was employed to build a membrane that was incorporated to an
314 extraction module and, later, to a sequential injection system. This system enabled to carry out
315 the on-line separation and enrichment of acidic proteins since PDDA allowed the surface charge
316 control. The developed tool was applied to the enrichment of BSA or human serum albumin in
317 5 min approximately that was a much lower time than the required with non-functionalized
318 MWCNTs [68]. The above-mentioned MWCNTs were highly reusable [75-77], being MWCNTs-
319 PDDA the one which provided the highest adsorption capacity. These works demonstrated the
320 great potential of MWCNTs in protein enrichment, achieving enrichment factors as high as 30
321 [76].

322 Metal-based NMs

323 Iron NPs (e.g. Fe_3O_4) have been applied for protein enrichment either directly
324 functionalized [78] or coated with a polymer [79] or silica [80,81]. Li's [78] and Sun's [79]
325 research groups employed different affinity ligands to functionalize MNPs. The use of
326 nitriloacetic acid (NTA) with attached Ni^{2+} enabled the specific enrichment of His-tag proteins in
327 just 30 s [78]. Due to the toxic effects of Ni^{2+}, other less toxic ions (Zn^{2+}, Cu^{2+}, and Fe^{2+}) were
328 later proposed despite they showed lower protein affinity. Sun et al. [79] developed a method to
329 synthesize MNPs coated with a polymeric mixture of PEG and carboxymethyl chitosan attaching
330 these metal ions. This material could be prepared at large scale in a simple and cost-effective
331 process. These MNPs were used to enrich lysozyme within 1 h. Interaction extent and mechanism
332 was controlled by pH and ionic strength modification. Moreover, in the case of MNPs with Zn^{2+}
333 and Fe^{2+}, the enrichment process did not produce the lysozyme denaturation, while in the case of
334 MNPs with Cu^{2+}, the desorbed lysozyme presented a slightly different structure from the original.
335 Other approach to enrich proteins is the use of $Fe_3O_4@SiO_2$ functionalized with different ligands
336 such as NH_2-guanidine groups [80] or IDA-Cu^{2+} [81]. Dong et al. [80] developed a solid-phase
337 extraction sorbent based on $Fe_3O_4@SiO_2$-NH_2-guanidine able to separate and preconcentrate

acidic proteins from basic proteins based on electrostatic forces and H bonds. They employed this sorbent to enrich BSA up to fifteen folds previously to its analysis by capillary electrophoresis, achieving detection limits of 45 ng/mL. Moreover, the applicability of these NPs was evaluated by the isolation and enrichment of BSA from a solution containing lysozyme and Cyto C. Finally, Fe_3O_4@SiO_2-IDA-Cu^{2+} NPs were successfully employed for selectively removing high abundant hemoglobin from both bovine and human blood in 6 h [81].

Noble metal-based NPs, which are non-magnetic, such as AuNPs [82-85] and Pd NPs [86], have also been used in the enrichment of standard proteins and proteins from real samples (see **Table 3**). Alwael el al. [82] designed pipette-tips functionalized with AuNPs-lectin as micro-extraction phase for the enrichment of a galactosylated glycoprotein from an *E. coli* cell lysate. To demonstrate the specificity of this material, it was used for the preconcentration of glycosylated proteins with different terminal sugars in a complex mixture containing non-glycosylated proteins. Bare AuNPs were also useful for protein enrichment [83]. The main advantage of this material was the effective protein enrichment in large-volume samples, where common enrichment methods (e.g. trichloroacetic acid precipitation) fail. Moreover, proteins adsorbed on NPs were analyzed by SDS-PAGE without any previous elution step and they were submitted to in-gel digestion. Moreover, AuNPs–(4-mercaptophenyliminomethyl)-2-methoxyphenol [84] were employed as extraction phase in the single drop microextraction of different proteins. Particularly, these NPs were used as multifunctional nanoprobes to serve, at the same time, as binary matrix, affinity and desalting probe in the MALDI-MS analysis of lysozyme in milk. Chiu et al. [85] employed AuNPs–transferrin antibody to both improve the sensitivity of the lateral-flow paper-based immunoassay and serve as colorimetric indicator. This system was employed to enrich transferrin from fetal bovine serum and urine, demonstrating is potential as diagnostic tool. On the other hand, Pd NPs functionalized with octadecanethiol [86] were employed for the selective and sensitive analysis of different proteins. Authors demonstrated that the optimal sample pH was that close to the protein pI, probably due to the enhancement of

hydrophobic interactions between proteins and octadecanethiol. Moreover, they found out that the addition of 1M NaCl enhanced signals intensity.

Other metal-based nanoparticles employed were ZnS-N_3 [87] and Co_3O_4 [88]. ZnS-N_3 NPs [87] resulted useful as multifunctional nanoprobes for the simultaneous enrichment and desalting of proteins for their subsequent MALDI-MS analysis or microwave-accelerated digestion. On the other hand, Co_3O_4 NPs [88] were employed in the enrichment and sensitive analysis of standard proteins and lysozyme from milk via liquid-liquid microextraction coupled with MALDI-MS. Both NPs [81, 82] enabled to enrich proteins in less than 1 h through electrostatic interactions and with preconcentration factors between 2 and 12.5.

Dendrimers

Despite the potential of dendrimers in protein enrichment, there is only one work employing carbosilane dendrimers for this purpose. They were used to enrich proteins from a complex sample, based on electrostatic interactions established between negatively charged carbosilane dendrimers and positively charged proteins [40]. **Figure 3.A** shows the image of the solutions prepared by mixing a myoglobin standard with increasing concentrations of third generation carboxylate-terminated carbosilane dendrimer at acidic pH. Protein solutions became white in presence of dendrimers due to the formation of a precipitate as consequence of the protein-dendrimer interactions. Moreover, **Figure 3.B** displays the profiles, obtained by SDS-PAGE, corresponding to a three-protein mixture (BSA, lysozyme, and myoglobin), the supernatants obtained after the treatment of this mixture with the dendrimer at 1:1, 1:8, and 1:20 ratios, and the precipitates obtained when using the 1:20 ratio and when using the conventional method to enrich proteins based on acetone precipitation. Results showed three clear bands corresponding to BSA, lysozyme, and myoglobin when no dendrimer was used (1:0) and more diffused bands in the supernatants obtained after protein-dendrimer mixtures were centrifuged. Bands intensity decreased up to a 1:20 protein:dendrimer ratio, where no protein band could be detected. At this ratio, precipitate showed the three bands corresponding to the proteins that were

not observed in the supernatant demonstrating that carboxylate-terminated carbosilane dendrimers were an effective methodology for protein enrichment/purification.

Nanocomposites

Shrivas et al. [89] employed MWCNTs@CdS@Cd^{2+} nanocomposite for the preconcentration of proteins through electrostatic interactions. Moreover, the exceptional photochemical properties of this nanocomposite enabled the efficient absorption of the laser energy when it was employed as matrix in MALDI-MS. Moreover, authors proved that this nanocomposite had more affinity toward ubiquitin than MWCNTs and CdS NPs, separately. In other approach, Xu et al. [90] synthesized TiO_2 nanotubes coated with carbon with large surface area. Their amphiphilic properties and their charge-tunable character allowed the extraction and enrichment of hydrophobic charged proteins. Moreover, their photocatalytic properties permitted the decomposition of undesirable not desorbed proteins and, thus, their reutilization. This platform was successfully employed to selectively enrich human serum albumin from human blood.

Liu et al. [91] synthesized core–shell structural MIP nanoparticles with assistant recognition polymer chains (ARPCs). In this approach, vinyl-modified silica NPs were the support, ARPCs were used as additional functional monomers, and the cloned bacterial protein was the template. This platform was applied to the enrichment of a natural low-abundance protein (immunoglobulin) in an extract of pig liver achieving an enrichment factor of 116.

Protein purification using NMs

The purification of proteins is a challenging process, which has the purpose of obtaining a pure protein for future applications. Different protein features (charge, molecular weight, hydrophobicity, post-translational modifications or the presence of tags) are the base of these purifications. Special attention has been paid to the purification of His-tag proteins since the use of DNA sequence specifying a chain of histidine residues (six to nine) is a recurrent approach to

produce recombinant proteins. **Table 4** groups those works using NMs for the purification of proteins in general and His-tag proteins. Works simultaneously used to extract and purify proteins, and already included in **Table 2**, have not been included in **Table 4**.

Carbon-based NMs

Purification of proteins employing carbon-based NMs is mainly based on electrostatic mediated interactions. Different commercial nanodiamonds, both bare and modified, were employed for the very fast purification of standard proteins [92]. On the other hand, carbon nanotubes treated with acid were used as chromatographic media for the purification of skim latex serum proteins [93,94].

Magnetic metal-based NMs

Like in protein extraction and enrichment, iron nanoparticles are mostly used (see **Table 4**), due to their easy separation and recovery, for the purification of proteins. Their functionalization has enabled the purification of a great variety of proteins. Indeed, MNPs synthesized by different methods, as supermagnetic iron oxide NPs (SPIONs) and MNPs prepared employing microemulsions (ME-MIONs) [95], resulted useful in the purification of up to 400-450 mg of a coagulant protein per g of NP, which supposed an efficient and versatile platform for the purification of *Moringa oleifera* coagulant like-proteins. Moreover, the activity of the coagulant protein was measured after the purification with the two different MNPs. Results revealed that the initial activity (24%) increased up to 84% and 90% when purifying with SPIONs and ME-MIONs, respectively. In other work, the coat of these magnetic iron NPs with trisodium citrate or silica [96] enabled the purification of that protein through electrostatic interactions in half the time. Nevertheless, while the use of MNPs functionalized with trisodium enabled to obtain the coagulant protein with an 80% activity, the use of MNPs coated with silica resulted in a lower protein activity. In both works, the disruption of interactions by increasing the ionic strength was required to the analysis of proteins by gel electrophoresis [95,96]. MNPs coated with polymers [97] or molecularly imprinted NPs [98] were also employed in protein purification. A

polymer-coated nanocluster [97] enabled the purification of 30 mg of Drosomycin per g of MNP yielding a high protein purification (90%). In the case of MIP-coated MNPs [92], the SDS-PAGE profiles demonstrated a high selectivity in the purification of BSA from a bovine blood sample. On the other hand, avidin and lysozyme have been the target of different purification processes [99-101] due to their interesting applications [102,103]. The stable interaction of avidin and iminobiotin has been of great utility for avidin purification [99]. These NPs permitted the purification of 225 mg of avidin from egg white per g of NPs. This purification process enabled to recover 92.8% of avidin with a purity of 98.5%. MNPs coated with poly(hydroxyethylmethacrylate-N-methacryloyl-(L)-tryptophan) (PHEMATrp) [100] or gold functionalized with 2-mercapto-5-benzimidazolesulfonic acid (MBISA) [101] were used in the purification of lysozyme from chicken egg white. PHEMATrp-coated NPs enabled a recovery of the 76% of the initial protein with a purity of 92%. In the case of Au-MBISA-coated NPs, the selectivity of the material towards lysozyme was demonstrated by SDS-PAGE. The development of the second approach enabled to reduce the purification time from 2 h to just 20 min, maintaining a good adsorption capacity and increasing the reusability. Moreover, Fe_3O_4 functionalized with oleate [104] was successfully employed to preconcentrate and remove the signal suppression observed when analyzing by mass spectrometry insulin, myoglobin, and Cyto C standards in presence of high salt concentrations. This platform enabled to reach low LOD values and very high adsorption capacities.

Despite electrostatic and hydrophobic interactions are the most usual driven forces in the purification with MNPs, the presence of more specific interactions makes more selective the process. As examples, glucose-lectin interactions, enzyme-substrate interactions, or metal affinity interactions were the base of the purification of specific proteins or groups of proteins [105-107] (see **Table 4**). The purification of the lectin concanavalin A was carried out in 5 min through its specific binding to a sugar [105]. The use of MNPs functionalized with glutathione enabled the purification in 10 min and almost the complete recovery of a glutathione S-tranferase-tag ubiquitin in different samples [106]. Finally, the interaction of laccase and MNPs through its

affinity with metal ions (Cu^{2+}) permitted a purification fold (final specific activity/initial specific activity) of 62.4 and an activity yield ((final Laccase activity/initial Laccase activity) x 100) of 108.9% [107].

Non-magnetic metal-based NMs

Although in less extent, AuNPs either functionalized with sugars [108] or embedded in a polymeric material [109] were also used for the purification of proteins. Lectins were purified from complex samples using AuNPs with sugars or in glycidyl methacrylate-co-ethylene dimethacrylate (GMA-co-EDMA). In the first case, proteins were then eluted by the addition of an inhibitory sugar, while in the second case, the elution was pH-controlled. In both cases, SDS-PAGE analysis demonstrated the effectiveness of the purification. Moreover, in the case of AuNPs-GMA-co-EDMA, Bradford analysis demonstrated the almost complete recovery of BSA and Cyto C after their purification.

Others

Additionally, polymer NPs have also been used for the purification of apolipoprotein A-I and other standard proteins based on affinity interactions [110,111]. In one case, copolymer NPs of N-isopropylacrylamide-N-tert-butylacrylamide were employed, while polystyrene latex NPs functionalized with different proteins, Concanavalin A or Protein G, were used in other work to coat the inner wall of capillaries. Copolymer NPs enabled the purification of 13 g of apolipoprotein A-I from human plasma per g of NPs. These NPs yielded a purification efficiency (percent purified protein compared to the nominal protein concentration) of 13%. On the other hand, the different functionalization of polystyrene NPs made possible the purification of either glycoproteins or immunoglobulins for their direct analysis by mass spectrometry or SDS-PAGE.

Histidine-tagged protein purification using NMs

493 Protein purification is usually limited by the low concentration of target proteins and the
494 low selectivity of the process. Protein engineering has made possible the overproduction of
495 proteins. For this purpose, most used approach consists of the introduction of a poly-histidine tag
496 (usually a chain with, at least, six consecutive histidine residues) to the C- or N- terminus of a
497 targeted protein, followed by protein expression in a bacterial system [112]. Moreover, the
498 tagging of proteins with histidine residues enables an enhancement in selectivity since histidine
499 presents a high affinity to metals.

500 Metal-based NMs

501 A widely used technique for the purification of His-tag proteins is by immobilized metal-
502 affinity chromatography [113] which is based on the interaction between metal ions (Ni^{2+}, Co^{2+},
503 Zn^{2+}, or Cu^{2+}) and amino acid residues, preferably histidine [114]. Based on the high affinity of
504 these metal ions and histidine, different NPs have been functionalized and applied for the
505 purification of proteins. Chen et al. functionalized silica-coated MNPs with zinc cations to
506 specifically purified His-tag proteins in 30 min, achieving a protein recovery of 83% [115].
507 Despite the good results observed with the direct attachment of metal cations to the NP surface,
508 an alternative approach based on the use of a chelating agent (mostly IDA and nitriloacetic acid
509 (NTA)) for the immobilization of the metal ion to the NP has also been described [116]. The
510 scheme of metal chelation with IDA and NTA and the interaction with His-tag proteins is shown
511 in **Figure 4**. The difference between them lies on the coordination number with the metal ion.
512 While IDA is trivalent, NTA is tetravalent and the interaction with the metal ion is stronger,
513 preventing the metal leakage during the purification process [112]. Although stability constant of
514 metal-NTA complex is higher than that of IDA complex, the higher density of binding sites and
515 lower imidazole concentration required for the elution, explain why some authors chose IDA as
516 the most suitable chelating agent for the purification of proteins. Moreover, the use of Fe_3O_4 as
517 magnetic core made possible the easy separation NPs from the sample and the coating with silica
518 [117] or PEG [118] improved NPs properties and stability. These two types of NPs attached nickel
519 cations and enabled the fast and efficient purification of His-tag proteins. Other chelator, used in

this case for the purification of a His-tag recombinant enhanced green fluorescent protein, was glycidyl methacrylate–iminodiacetic acid (GMA–IDA). This quelator was polymerized with divinyl benzene and styrene in presence of the Fe_3O_4 NPs and loaded with Cu^{2+}, Ni^{2+}, or Zn^{2+} cations [119]. The nature of the metal cation attached to GMA–IDA affected protein recovery and purification efficiency, being copper cation the one providing the better results (recovery = 70.4%; purification factor = 12.3). These NPs enabled the purification of green fluorescent protein in just 10 min, while IDA and NTA used to require higher times. Indeed, Fe_3O_4–NTA-Ni^{2+} NPs were employed to purify His-tag recombinant proteins from *E. coli* o *P. pastoris* lysates in times ranging from 20 min to 12 h, depending on the targeted protein [120-122]. Moreover, the use of a bis-NTA instead of NTA enabled the interaction of proteins with the double number of metal ions. This approach was applied to the purification a His-tag mouse endostatin resulting in no activity lose [123]. These NPs were reusable and showed adsorption capacities between 61.3 and 230 mg protein/g NPs. Moreover, the coating of the magnetic core with silica provided a protective layer against oxidation and also enabled NP functionalization [124-128]. Furthermore, Liao et al. mixed silica with boron to reduce the iron leakage produced after separation [124]. In other occasions, silica was functionalized with polymers to increase the number of NTA-metal bonds [125,127]. The use of these NPs enabled to recover 77% of the initial protein [125]. Moreover, purification times when employing silica-coated NPs did not exceed 1 h, being the NPs functionalized with polymers the ones enabling the shorter purification times (5-10 min) [125,127].

Other molecules such as EDTA [129], aspartic acid [130], phenanthroline [131], and terpyridine receptor [132] have also been used to bind divalent metal ions and applied to the purification of His-tag proteins. In fact, MNPs functionalized with EDTA enabled the recovery of the 93% of an His-tag protein with a 96% of purity [129]. Phenanthroline [131] and terpyridine receptor [132] resulted in a purification fold close to 1 and an activity yield of 100%. In both cases, the efficiency of the purification was confirmed by SDS-PAGE analysis. Moreover,

546 polymers as polydopamine were also used for His-tag protein purification [133], enabling the
547 purification of an His-tag red fluorescent protein in just 5 min.

548 Albeit the divalent metal ion-histidine interaction is very common for His-tag protein
549 purification, other approaches using two metal ions have successfully been applied. Ni-$ZnFe_2O_4$
550 NPs were employed to purify His-tag proteins in *E. coli* [134]. In this kind of NPs, iron was
551 concentrated in the NPs core while zinc and nickel did it in the NPs surface. This fact may promote
552 the adsorption of proteins to de NPs surface.

553 There is only one work that used non-magnetic NPs for the purification of His-tag proteins.
554 In fact, Ni NPs enabled a very fast His-tag protein purification from and *E. coli* cell lysate and
555 could be reused for 4 cycles [135].

556 Nanocomposites

557 A great variety of nanocomposites enabled the His-tag protein purification from *E. coli*.
558 For example, Man-Hua et al. [136] synthesized carbon nanospheres from glucose, introduced
559 MNPs in their pores, and, finally, conjugated NTA-Ni^{2+} to this system. The use of C@Fe_3O_4–
560 NTA-Ni^{2+} NPs enabled the His-tag protein purification in 2 h and the separation of NPs either by
561 a magnet or by centrifugation. In other approach, Fe_3O_4@Au–ANTA-Co^{2+} NPs [137] were
562 employed for His-tag protein purification in a much lower time (10 min) and enabling 4 cycles
563 reuse. Despite this, the amount of adsorbed protein was the third part that obtained with
564 C@Fe_3O_4–NTA-Ni^{2+} NPs. A more sophisticated approach based on porous silica-coated MNPs
565 with NiO NPs formed in their pores also enabled the selective purification of His-tag proteins in
566 10 min [138]. The use of $NiFe_2O_4$ NPs coated with a shell of $NiAl_2O_4$ [139] resulted in a higher
567 purification time (30 min) but NPs were reused for 20 cycles obtaining a high adsorption capacity.
568 Moreover, studies on the eluted proteins demonstrated no toxicity due to nickel leakage and no
569 change of proteins structure. Despite much less usual than the histidine-tag, methionine-tag and
570 cysteine-tag have also been employed for the purification of recombinant proteins.
571 Fe_3O_4@AuNPs-phosphorylcholine NPs [140] were applied to the purification of proteins based

572 on the specific binding between AuNPs and these amino acids through Au-S bonds. The purpose
573 of the functionalization with phosphorylcholine was the reduction of the non-specific binding
574 without losing the specific adsorption capacity on Fe_3O_4@AuNPs NPs.

575

576

577 Others

578 Other kind of NPs, polystyrene latex NPs, were functionalized with IDA-Ni^{2+} in the inner
579 wall of a capillary [111]. This system allowed a His-tag protein purification for its subsequent
580 analysis by mass spectrometry.

581

582 **PROTEIN DIGESTION USING NANOMATERIALS**

583 Protein digestion is a usual step in protein sample preparation although it is not always
584 required. It is a tedious, time-consuming, and difficult to automate process. Protein digestion is
585 needed in proteomics (bottom-up method) but also for other purposes such as obtaining bioactive
586 peptides or to carry out any catalytic process within biotechnology. Most widely employed
587 enzyme for protein digestion in proteomic analysis is trypsin, which is a cheap and selective
588 enzyme with a high activity. This enzyme cleaves the protein next to arginine or lysine residues
589 but not after proline residues. Thus, it generates peptides with these basic amino acids in the C-
590 terminus enabling peptide ionization and fragmentation by mass spectrometry [141]. Less specific
591 proteases (Alcalase, Thermolysin, Flavourzyme, etc.) are required when protein digestion is
592 carried out to obtain bioactive peptides, usually short peptides [142-147].

593 NMs can be used in protein digestion with two purposes (see **Figure 5**). NMs can be used
594 to bind or adsorb proteins previously to the addition of the enzyme (**Figure 5A**). In many of these
595 cases, NMs are employed in combination with microwaves, since they can act as radiation
596 sorbent. On the other hand, NMs can be used to immobilize the own enzyme (**Figure 5B**),

reducing enzyme autolysis and loss of activity [148], and enabling the recovery of the enzyme for next digestions [149]. All approaches using NPs for protein digestion are listed in **Table 5**.

NMs used to support proteins for their digestion

On-bead digestion

The nanometric size of some materials makes them capable of adsorbing high amounts of proteins. Moreover, as previously discussed, NPs can selectively extract, concentrate and/or desalt proteins from a sample. Another advantage of NPs is the fact that, in many cases, the adsorbed proteins can be on-bead-digested not requiring the previous separation from NPs. Additionally, digested extracts can be directly analyzed by MALDI-MS since NPs do not interference in the desorption/ionization process due to their small size. For example, Fe_3O_4-oleate NPs [104] and oMWCNT@Fe_3O_4 NPs [71] were used for the on-bead tryptic digestion of proteins that had previously been concentrated and/or desalted on the own beads. In these cases, proteins, adsorbed on the NPs surface, were reduced, alkylated, and digested with trypsin, employing digestion times up to 24 h. In the case of Fe_3O_4-oleate NPs [98], it was possible to match 12 peptides, although 9 of them presented missed cleavages. The use of AuNPs [150] permitted not only the reduction of digestion times from 24 h to 6 h, but the quantification of bound BSA after its digestion with trypsin, addition of an isotope-labeled internal reference peptide standard, and mass spectrometry analysis. An even lower digestion time was required when proteins were retained in fourth-generation PAMAM dendrimers. In this case, dendrimers were incorporated in a chip platform enabling protein adsorption via antigen-antibody interactions [151]. This method was applied to the analysis of BSA in a standards mixture and in human serum and the analysis of proteins from an *E. coli* cell lysate and, in all cases, tryptic digestion was accomplished in 3 h. Main limitation was the obtained sequence coverage that did not exceed 33%. In a more recent

work using surface-oxidized nanodiamonds [152], digestion times were reduced to just 5 min but, again, sequence coverage was limited (23-30%).

Different efforts based on the application of different radiations have been performed to reduce digestion times and to increase sequence coverage.

Microwave-assisted digestion

Digestion of proteins is highly accelerated when using microwaves that, in combination with protein adsorption on NPs, has enabled to reduce digestion times. The first time that magnetite (Fe_3O_4) NPs were employed for microwave-assisted tryptic digestion of proteins was in 2007 [153]. In this work, Chen et al. demonstrated that the reduction in digestion time was due to different facts: MNPs absorb microwaves radiation enabling their fast heating and they can also adsorb proteins via electrostatic interactions allowing their concentration and denaturation and making them more susceptible to trypsin digestion. This enabled Cyto C and myoglobin digestion in less than 1 min with high sequence coverage, although the percentage of matched peptides with missed cleavages was also high. After this first example, other MNPs (Fe_3O_4-NTA-Ni^{2+} NPs [78], Fe_3O_4@SiO_2-APTES NPs [154] and Fe_3O_4@ZnO NPs [155]) were also employed for the microwave-assisted tryptic digestion of different proteins. In all cases, proteins were firstly concentrated on the NP surface by affinity or electrostatic interactions and, then, digested in less than 2 min by microwaves assistance. It is important to highlight the high sequence coverage obtained with these NPs, reaching 100% in the case of Cyto C [154]. Not just MNPs were employed for enzymatic digestion, but also TiO_2 NPs [156,157], ZnS-N_3 NPs [87], Pt NPs [158] or MWCNT@CdS@Cd^{2+} NPs [89]. They achieved the digestion of different standard proteins and lysozyme and phosphoproteins from milk in less than 1 min. Particularly, TiO_2 NPs [156,157] were an excellent material for the enhancement of digestion efficiency, sequence coverage and sensitivity when analyzing by mass spectrometry with different ionization modes.

NIR-assisted digestion

649 The application of near infrared (NIR) radiation has also enabled to reduce digestion times.
650 The use of glass@AuNPs in combination with NIR radiation was used to digest different proteins,
651 including human serum proteins, in less than 5 min [159]. The rapid raise in surface temperature
652 due to NIR radiation enabled the acceleration of both in-solution and in-gel digestions. The in-
653 solution digestion of Cyto C resulted in a sequence coverage of 95%, even though more than the
654 80% of matched peptides contained missing cleavages. In the case of in-gel digestion, just 12%
655 of sequence coverage was achieved, similar to the obtained by in-solution digestion. This fact is
656 probably due to the need of a previous protein denaturation step. The use of glass@AuNPs for
657 the NIR-assisted in-gel digestion of a real complex sample (human serum) enabled a sequence
658 coverage similar to that obtained when digesting in-gel for 16 h and much higher than that
659 obtained when the digestion was carried out during 5 min at room temperature.

660 **NMs used for the immobilization of enzymes**

661 Magnetic metal-based NMs

662 The immobilization of trypsin on the NPs surface supposes great advantages from the point
663 of view of efficiency and automation. First attempts of enzyme immobilization consisted of the
664 direct functionalization of MNPs with trypsin [160-164] (see **Table 5**). The simple handling of
665 these MNPs with a magnet made easy the separation process. The digestion rate was so high,
666 especially at high temperatures [161], that it was not required the previous reduction and
667 alkylation of targeted proteins [160,161]. Moreover, NPs could be reused up to 9 times [160,161]
668 and required low sample volumes [161]. Additionally, the combination with microwave radiation
669 enabled to reduce to a few seconds the digestion time [162,163]. Commercial MNPs have also
670 been directly functionalized with trypsin enabling digestions in just 1 min but without reuse
671 possibility [164]. High sequence coverages were observed in most cases. It is highlightable the
672 work of Li et al. [160] using Fe_3O_4-trypsin NPs, that identified a 76, 46, and 90% of Cyto C, BSA,
673 and myoglobin sequences, respectively, and the work using commercial MNPs [158], that
674 identified the 45% of the casein sequence and the complete sequence of insulin.

675 Other strategy has been the coating of the MNPs either with polymers or silica before
676 enzyme functionalization which resulted in a higher protection and an easier functionalization of
677 NPs. There are different examples using Fe_3O_4@SiO_2 NPs directly functionalized with trypsin
678 with digestion times ranging from 1-16 h [165-167] (see **Table 5**). Lee et al. [165] observed that
679 the long digestion time required when digestion was carried out at atmospheric pressure could be
680 reduced to just a few minutes when pressure cycles were applied, making these NPs highly
681 reusable. Moreover, this reduction of digestion time came along with an increase in the proteins
682 sequence coverage. In other approaches, Fe_3O_4@SiO_2 NPs were coated with polymeric chains
683 before the immobilization of trypsin [168,169]. These chains enabled the immobilization of a
684 huge amount of enzyme and, thus, a faster digestion (1 or 2 min) compared to the 12-20 h of a
685 free-enzyme digestion. Moreover, in the case of BSA digestion, the sequence coverage obtained
686 was higher than the obtained when free-trypsin digestion was carried out. On the other hand, the
687 immobilization of trypsin in hydrophilic or hydrophobic polymeric chains and the combination
688 of these two kinds of NPs allowed the comprehensive identification of peptides from yeast
689 proteins and mouse liver membrane proteins [169]. Shen et al. [170] used the same strategy
690 introducing polymer brushes of poly(glycidyl methacrylate) but, in this case, directly into the
691 Fe_3O_4 NPs surface. These NPs achieved the Cyto C digestion in 1 min at 37 ^{0}C and reduced this
692 time to just 15 s when digestion was assisted by microwaves (without losing sequence coverage).
693 In both cases, NPs could still be reused. Meanwhile, Cheng et al. [171] coated Fe_3O_4 NPs with
694 another polymer (polydopamine) and performed the digestion of Cyto C, myoglobin, and BSA
695 standards within 30 min obtaining high sequence coverages (55-92%). Moreover, digestion
696 resulted effective even using very low protein concentrations (5 ng/μL). As example, **Figure 6**
697 displays MALDI-TOF spectrum corresponding to Cyto C digestion with the magnetic enzyme
698 nanosystem for 30 min **(A)** and compares it with the spectra obtained employing in-solution
699 digestion at 30 min **(B)** and 12 h **(C)**. Results showed that the magnetic enzyme nanosystem
700 provided much better results in 30 min than in the in-solution digestion and similar to the obtained
701 with a longer in-solution digestion. MNPs different from Fe_3O_4 NPs were also employed for
702 trypsin immobilization, as γ-Fe_2O_3 NPs, that were entrapped within polymeric nanofibers to

703 generate an easy-separable digestion support [172]. This reusable nanomaterial enabled the tryptic
704 digestion of an enolase in 10 min.

705 Immobilized enzymes have also been employed to produce bioactive peptides. There are
706 two works focused to obtain peptides from casein with either antioxidant [173] or angiotensin-
707 converting enzyme inhibitory [174] capacity. The digestion of casein with *Penicillium*
708 *aurantiogriseum* protease immobilized on glutaraldehyde-activated MNPs yielded peptides with
709 antioxidant activity within 45 min. The activation of Fe_3O_4-polyaniline with glutaraldehyde
710 enabled the covalent binding of the protease and, thus, a major stability. On the other hand,
711 *Aspergillus oryzea* protease was encapsulated, together with MNPs, within nanospheres prepared
712 by the silicification of PAMAM dendrimers. The protease encapsulation significantly enhanced
713 its resistance to thermal and ultrasonic treatment. This NM allowed to obtain angiotensin-
714 converting enzyme inhibitory peptides in 3 h. In this case, the application of ultrasounds made
715 possible the acceleration of the process up to 30 min without losing peptides activity.

716 Non-magnetic metal-based NMs

717 Other materials employed for enzyme immobilization were AuNPs, AgNPs, CNTs, GO,
718 dendrimers, zeolites or silica (see **Table 5**). Safdar et al. [175] built two open tubular
719 microreactors with trypsin immobilized on AuNPs which enabled to accelerate about 150 times
720 a tryptic digestion. The difference between the two microreactors was on the binding of trypsin
721 to the AuNPs: direct functionalization or functionalization through PEG chains. Both
722 microreactors enabled similar, or even better, proteins sequence coverages than the conventional
723 digestion. In other approach, Gogoi et al. [176] embedded AgNPs into a polymeric film and
724 attached trypsin through covalent bonds. This synthesized matrix was a more efficient digestion
725 support than the free enzyme or the enzyme immobilized directly on the film and allowed BSA
726 digestion in 50 min.

727 Although trypsin is the most common enzyme employed for protein digestion in proteomic
728 analysis, in some cases it can produce very short peptides resulting in an incomplete sequence

729 coverage. An alternative enzyme as pepsin could be useful in these cases. Höldrich et al. [177]
730 synthesized a recyclable nanobiocatalyst by the immobilization of pepsin on AuNPs through
731 PEG. Authors demonstrated that this immobilization retained enzyme activity and yielded
732 proteins sequence coverages as good as the obtained with free-pepsin digestion and in shorter
733 times. Nevertheless, digestion time was much higher (4 h) than the obtained for the same proteins
734 and NPs when digesting with trypsin [169].

735 Nanocomposites

736 MNPs have also been employed for the synthesis of a nanocomposite made of four
737 components [178]. In this case, the immobilization of trypsin on polyaniline coated
738 MWCNTs/Fe_3O_4 composites enabled the digestion of standard proteins yielding a good sequence
739 coverage (46-81%) and being reusable for 5 cycles. On the other hand, the immobilization of
740 trypsin on carbon-based materials – PAMAM dendrimers nanocomposites was another approach
741 for protein digestion. Firstly, Zhang et al. [179] immobilized trypsin to fourth-generation
742 PAMAM dendrimers attached to carbon nanotubes and employed them for the fast on-plate
743 digestion of lysozyme and Cyto C without any tedious pretreatment of proteins. Later, Jiang et al.
744 [180] grafted second-generation PAMAM dendrimers to GO and immobilized the enzyme on
745 them. Since this material did not interfere with MALDI-MS analysis, it was used for the on-plate
746 digestion of proteins, showing good sensitivity even with trace protein concentrations. Both works
747 [173,174] permitted the identification of proteins with elevated sequence coverage in 15 min,
748 although the one using CNTs resulted in a higher value for Cyto C. Other approach involved the
749 use of poly(methyl methacrylate) microchips where microchannels were modified with silicalite
750 zeolite [181]. The trypsin immobilization on these microchannels enabled the ultrafast digestion
751 of Cyto C and BSA in less than 5 s.

752 Others

753 Despite silica has been employed as coating of different NPs, the direct immobilization of
754 enzymes on silica has also been performed. Indeed, trypsin, immobilized on mesoporous silica

nanotubes, enabled the digestion of α-casein within just 3 min [182]. This fast digestion had as consequence the formation of large peptides and, thus, resulted in an increase in phosphopeptide relative abundance. On the other hand, the coating of silica with cellulose and posterior immobilization of trypsin resulted in highly reusable and thermally stable NPs able to carry out the digestion of casein, BSA, Cyto C, and collagen in 30 min [183]. Both silica-based NMs enabled the identification of proteins with sequence coverages higher than 60%.

CONCLUSIONS AND FUTURE PERSPECTIVES

Nanomaterials are increasingly employed in the different steps of protein sample preparation. All these applications are based on a variety of interactions that can be established between proteins and nanomaterials such as electrostatic, hydrophobic, or affinity interactions. Current efforts on the field are devoted to the development of new nanomaterials or functionalities improving the effectiveness of the method. They mainly consist of the enhancement of sensitivity and selectivity, the increase of the adsorption capacity, the improvement in the nanomaterials handling, and the reduction of time. For that reason, future researches should be focused on the development of novel affinity probes enabling the easy, fast, cost-effective, and complete extraction, enrichment, purification, or digestion of proteins. All these improvements can enhance protein sample preparation in the identification of specific proteomes, obtaining of bioactive peptides, quantification of proteins, control food authenticity, or in the evaluation of the presence of protein allergens, among others.

774 **ACKNOWLEDGEMENTS**

775 This work was supported by the Spanish Ministry of Economy and Competitiveness (ref.
776 AGL2016-79010-R) and the Comunidad Autónoma of Madrid (Spain) and European
777 funding from FEDER program (project S2013/ABI-3028, AVANSECAL-CM). E.G.-G.
778 thanks the University of Alcalá for her pre-doctoral contract.

779

780 **REFERENCES**

781 [1] Wang, W., Tai, F., and Chen, S. (2008) Optimizing protein extraction from plant tissues
782 for enhanced proteomics analysis. *J. Sep. Sci.,* 31: 2032-2039.

783 [2] Wu, X., Gong, F., and Wang, W. (2014) Protein extraction from plant tissues for 2DE and
784 its application in proteomic analysis. *Proteomics*, 14: 645-658.

785 [3] Boland, M.J. (2002) Aqueous two-phase extraction and purification of animal proteins.
786 *Mol. Biotechnol.,* 20: 85-93.

787 [4] Feist, P., and Hummon, A.B. (2015) Proteomic challenges: Sample preparation techniques
788 for microgram-quantity protein analysis from biological samples. *Int. J. Mol. Sci.,* 16:
789 3537-3563.

790 [5] Geciova, J., Bury, D., and Jelen, P. (2002) Methods for disruption of microbial cells for
791 potential use in the dairy industry - a review. *Int. Dairy J.*, 12:541-553.

792 [6] Barraclough, D., Obenland, D., Laing, W., and Carroll, T. (2004) A general method for
793 two-dimensional protein electrophoresis of fruit samples. *Postharvest Biol. Technol.*,
794 32:175-181.

795 [7] Wu, F.S. and Wang, M.Y. (1984) Extraction of proteins for sodium dodecyl-sulfate
796 polyacrylamide-gel electrophoresis from protease-rich plant-tissues. *Anal.*
797 *Biochem.*,139:100-103.

798 [8] Wessel, D., Flugge, U.I. (1984) A method for the quantitative recovery of protein in dilute-
799 solution in the presence of detergents and lipids. *Anal. Biochem.*,138:141-143.

800 [9] Englard, S. and Seifter, S. (1990) Precipitation techniques. *Meth. Enzymol*., 182: 285-300.

801 [10] Walls, D., Cooney, G., and Loughran, S.T. (2017) A synopsis of proteins and their
802 purification. *Methods Mol. Biol.,* 1485: 3-14.

803 [11] Honig, W. and Kula, M.R. (1976) Selectivity of protein precipitation with polyethylene-
804 glycol fractions of various molecular-weights. *Anal. Biochem.*, 72:502-512.

805 [12] Zhang, Y., Gao, P., Xing, Z., Jin, S., Chen, Z., Liu, L., Constantino, N., Wang, X., Shi, W.,
806 Yuan, J.S., and Dai, S.Y. (2013) Application of an improved proteomics method for

807 abundant protein cleanup: Molecular and genomic mechanisms study in plant defense. *Mol.*
808 *Cell. Proteomics*, 12:3431-3442.
809 [13] Switzar, L., Giera, M., and Niessen, W.M.A. (2013) Protein digestion: An overview of the
810 available techniques and recent developments. *J. Proteome Res.,* 12: 1067-1077.
811 [14] Yokoyama, T. (2012) Basic properties and measuring methods of nanoparticles. In: Nogi,
812 K., Hosokawa, M., Naito, M., and Yokoyama, T. (Eds.), *Nanoparticle Technology*
813 *Handbook (second ed.)*, Elsevier: Oxford, UK. pp. 5-49.
814 [15] Vajtai, R. (2013) Science and engineering of nanomaterials. In: Vajtai R. (Ed.), *Springer*
815 *Hanbook of Nanomaterials*, Springer Science & Business Media: Heidelberg, Germany.
816 pp. 1-36.
817 [16] Cao, G. and Wang, Y. (2011) Characterization and properties of nanomaterials. In: Cao, G.
818 and Wang Y. (Eds.), *Nanostructures and nanomaterials: Synthesis, properties, and*
819 *applications (second ed.)*, World Scientific Publishing Company: Singapore. pp. 433-508.
820 [17] Roy, A. and Bhattacharya, J. (2015) Introduction to nanotechnology. In: Roy, A. and
821 Bhattacharya, J. (Eds.), *Nanotechnology in industrial wastewater treatment (first ed.)*, IWA
822 Publishing: London, UK. pp. 5-10.
823 [18] Bashir, S. and Liu, J. (2015) Nanomaterials and their applications. In: Bashir, S. and Liu,
824 J. (Eds.), *Advanced Nanomaterials and their applications in renewable energy (first ed.)*,
825 Elsevier: Waltham, MA, USA. pp. 1-50.
826 [19] Ma, H., Diamond, S., Hinkley, G., and Kuperberg, J.M. (2015) Nanotoxicology. In:
827 Roberts, S.M., James, R.C., and Williams, P.L. (Eds.), *Principles of toxiclogy:*
828 *Environmental and industrial applications, (third ed.)*, John Wiley & Sons: Hoboken, New
829 Jersey, USA. pp. 359-372.
830 [20] Coro, J., Suárez, M., Silva, L.S.R., Eguiluz, K.I.B., and Salazar-Banda, G.R. (2016)
831 Fullerene applications in fuel cells: A review. *Int. J. Hydrog. Energy*, 41: 17944-17959.
832 [21] Mohajeri, A. and Omidvar, A. (2015) Fullerene-based materials for solar cell applications:
833 design of novel acceptors for efficient polymer solar cells - a DFT study. *Phys. Chem.*
834 *Chem. Phys.,* 17: 22367-22376.

835 [22] Lai, Y., Cheng, Y., and Hsu, C. (2014) Applications of functional fullerene materials in
836 polymer solar cells. *Energy Environ. Sci.,* 7: 1866-1883.
837 [23] Mousavi, S.Z., Nafisi, S., and Maibach, H.I. (2016) Fullerene nanoparticle in
838 dermatological and cosmetic applications. *Nanomed.-Nanotechnol. Biol. Med.*, 13: 1071-
839 1087.
840 [24] Yang, X., Ebrahimi, A., Li, J., and Cui, Q. (2014) Fullerene-biomolecule conjugates and
841 their biomedicinal applications. *Int. J. Nanomed.,* 9: 77-92.
842 [25] Zhu, C., Du, D., and Lin, Y. (2017) Graphene-like 2D nanomaterial-based biointerfaces for
843 biosensing applications. *Biosens. Bioelectron*., 89: 43-55.
844 [26] Yu, X. Zhang, W., Zhang, P., and Su, Z. (2017) Fabrication technologies and sensing
845 applications of graphene-based composite films: Advances and challenges. *Biosens.*
846 *Bioelectron.,* 89: 72-84.
847 [27] Yu, F., Wang, C., and Ma, J. (2016) Applications of graphene-modified electrodes in
848 microbial fuel cells. *Materials*, 9: 807.
849 [28] Shi, L., Chen, J., Teng, L., Wang, L., Zhu, G., Liu, S., Luo, Z., Shi, X., Wang, Y., and Ren,
850 L. (2016) The antibacterial applications of graphene and its derivatives. *Small*, 12: 4165-
851 4184.
852 [29] Jakubus, A., Paszkiewicz, M., and Stepnowski, P. (2017) Carbon nanotubes application in
853 the extraction techniques of pesticides: A review. *Crit. Rev. Anal. Chem*., 47: 76-91.
854 [30] Kumar, S., Rani, R., Dilbaghi, N., Tankeshwar, K., and Kim, K. (2017) Carbon nanotubes:
855 a novel material for multifaceted applications in human healthcare. *Chem. Soc. Rev*., 46:
856 158-196.
857 [31] Amenta, V. and Aschberger, K. (2015) Carbon nanotubes: potential medical applications
858 and safety concerns. *Wiley Interdiscip. Rev.-Nanomed. Nanobiotechnol*., 7: 371-386.
859 [32] Madhumitha, G., Elango, G., and Roopan, S.M. (2016) Biotechnological aspects of ZnO
860 nanoparticles: overview on synthesis and its applications. *Appl. Microbiol. Biotechnol*.,
861 100: 571-581.

862 [33] Senthilkumar, S.R. and Sivakumar, T. (2014) Green tea (*Camellia sinensis*) mediated
863 synthesis of zinc oxide (ZnO) nanoparticles and studies on their antimicrobial activities.
864 *Int. J. Pharm. Pharm. Sci*., 6: 461-465.
865 [34] Zhang, Z. and Xiong, H. (2015) Photoluminescent ZnO nanoparticles and their biological
866 applications. *Materials*, 8: 3101-3127.
867 [35] Shi, L., Li, Z., Zheng, W., Zhao, Y., Jin, Y., and Tang, Z. (2014) Synthesis, antibacterial
868 activity, antibacterial mechanism and food applications of ZnO nanoparticles: A review.
869 *Food Addit. Contam. Part A-Chem*., 31: 173-186.
870 [36] Majdalawieh, A., Kanan, M.C., El-Kadri, O., and Kanan, S.M. (2014) Recent advances in
871 gold and silver nanoparticles: Synthesis and applications. *J. Nanosci. Nanotechnol*. 14:
872 4757-4780.
873 [37] Long, N.V., Thi, C.M., Yong, Y., Cao, Y., Wu, H., and Nogami, M. (2014) Synthesis and
874 characterization of Fe-based metal and oxide based nanoparticles: Discoveries and research
875 highlights of potential applications in biology and medicine. *Recent Pat. Nanotechnology*,
876 8: 52-61.
877 [38] Biju, V., Itoh, T., Anas, A., Sujith, A., and Ishikawa, M. (2008) Semiconductor quantum
878 dots and metal nanoparticles: syntheses, optical properties, and biological applications.
879 *Anal. Bioanal. Chem*., 391: 2469-2495.
880 [39] Kalhapure, R.S., Kathiravan, M.K., Akamanchi, K.G., and Govender, T. (2015)
881 Dendrimers - from organic synthesis to pharmaceutical applications: an update. *Pharm.*
882 *Dev. Technol*., 20: 22-40.
883 [40] González-García, E., Maly, M., de la Mata, F.J., Gómez, R., Marina, M.L., and García,
884 M.C., (2016) Proof of concept of a "greener" protein purification/enrichment method based
885 on carboxylate-terminated carbosilane dendrimer-protein interactions. *Anal. Bioanal.*
886 *Chem*., 408: 7679-7687.
887 [41] Noriega-Luna, B., Godínez, L.A., Rodríguez, F.J., Rodríguez, A., Zaldívar-Lelo de Larrea,
888 G., Sosa-Ferreyra, C.F., Mercado-Curiel, R.F., Manríquez, J., and Bustos, E. (2014)

889 Applications of dendrimers in drug delivery agents, diagnosis, therapy, and detection. *J.*
890 *Nanomater.,* Article ID: 507273.
891 [42] Ke, Y.C. and Stroeve, P. Background on polymer-layered silicate and silica
892 nanocomposites. In: Ke, Y.C. and Stroeve, P. (Eds.), *Polymer-layered silicate and silica*
893 *nanocomposites (first ed.)*, Elsevier, Amsterdam, The Netherlands, 2005, pp. 1-67.
894 [43] Chen, C., Yu, W., Liu, T., Cao, S., and Tsang, Y. (2017) Graphene oxide/WS_2/Mg-doped
895 ZnO nanocomposites for solar-light catalytic and anti-bacterial applications. *Solar Energy*
896 *Mater. Solar Cells*, 160: 43-53.
897 [44] Mallakpour, S. and Khadem, E. (2016) Carbon nanotube-metal oxide nanocomposites:
898 Fabrication, properties and applications. *Chem. Eng. J.*, 302: 344-367.
899 [45] Peng, Q. and Mu, H. (2016) The potential of protein-nanomaterial interaction for advanced
900 drug delivery. *J. Controlled Release*, 225: 121-132.
901 [46] Bendicho, C., Costas-Mora, I., Romero, V., and Lavilla, I. (2015) Nanoparticle-enhanced
902 liquid-phase microextraction. *Trac-Trends Anal. Chem*., 68: 78-87.
903 [47] Sanagi, M.M., Hussain, I., Ibrahim, W.A.W., Yahaya, N., Kamaruzaman, S., Abidin
904 N.N.Z., and Ali, I. (2016) Micro-extraction of xenobiotics and biomolecules from different
905 matrices on nanostructures. *Sep. Purif. Rev*., 45: 28-49.
906 [48] Chan, K. and Ng, T.B. (2011) Isolation and detection of proteins with nano-particles and
907 microchips for analyzing proteomes on a large scale basis. *Protein Pept. Lett*., 18: 423-433.
908 [49] Lin, J., Tseng, W. (2012) Gold nanoparticles for specific extraction and enrichment of
909 biomolecules and environmental pollutants. *Rev. Anal. Chem.*, 31: 153-162.
910 [50] Gao, J., Gu, H., and Xu, B. (2009) Multifunctional magnetic nanoparticles: Design,
911 synthesis, and biomedical applications. *Acc. Chem. Res*., 42: 1097-1107.
912 [51] Gao, M., Deng, C., and Zhang, X. (2011) Magnetic nanoparticles-based digestion and
913 enrichment methods in proteomics analysis. *Expert Rev. Proteomics*, 8: 379-390.
914 [52] Cao, M., Li, Z., Wang, J., Ge, W., Yue, T., Li, R., Colvin, V.L., and Yu, W.W. (2012) Food
915 related applications of magnetic iron oxide nanoparticles: Enzyme immobilization, protein
916 purification, and food analysis. *Trends Food Sci. Technol*., 27: 47-56.

[53] Yildiz I., (2016) Applications of magnetic nanoparticles in biomedical separation and purification, *Nanotechnol. Rev*., 5: 331-340.

[54] Najam-ul-Haq, M., Rainer, M., Schwarzenauer, T., Huck, C.W., and Bonn, G.K. (2006) Chemically modified carbon nanotubes as material enhanced laser desorption ionisation (MELDI) material in protein profiling. *Anal. Chim. Acta,* 561: 32-39.

[55] Du, Z., Liu, M., and Li, G. (2013) Development of a membrane solid-phase extraction method based on polyethyleneimine modified MWNTs for on-line extraction and preconcentration of acidic proteins in serum samples. *Anal. Methods*, 5: 4921-4926.

[56] Shukoor, M.I., Natalio, F., Tahir, M.N., Ksenofontov, V., Therese, H.A., Theato, P., Schroeder, H.C., Mueller, W.E.G., and Tremel, W. (2007) Superparamagnetic gamma-Fe_2O_3 nanoparticles with tailored functionality for protein separation. *Chem. Commun*., 4677-4679.

[57] Wang, B., Wang, X., Wang, J., Xue, X., Xi, X., Chu, Q., Dong, G., and Wei, Y. (2016) Amino acid-based ionic liquid surface modification on magnetic nanoparticles for the magnetic solid-phase extraction of heme proteins. *RSC Adv.*, 6: 105550-105557.

[58] Liu, Y., Li, Y., and Wei, Y. (2014) Highly selective isolation and purification of heme proteins in biological samples using multifunctional magnetic nanospheres. *J. Sep. Sci*., 37: 3745-3752.

[59] Pardo, A., Mespouille, L., Dubois, P., Duez, P., Blankert, B. (2012) Targeted extraction of active compounds from natural products by molecularly imprinted polymers, *Cent. Eur. J. Chem.*, 10: 751-765.

[60] Li, N., Qi, L., Shen, Y., Qiao, J., and Chen, Y. (2014) Novel oligo(ethylene glycol)-based molecularly imprinted magnetic nanoparticles for thermally modulated capture and release of lysozyme. *ACS Appl. Mater. Interfaces*, 6: 17289-17295.

[61] Arnau, J., Lauritzen, C., Petersen, G.E., and Pedersen, J. (2006) Current strategies for the use of affinity tags and tag removal for the purification of recombinant proteins. *Protein Expr. Purif*., 48: 1-13.

[62] Gaberc-Porekar, V. and Menart, V. (2005) Potential for using histidine tags in purification of proteins at large scale. *Chem. Eng. Technol*., 28: 1306-1314.

[63] Yao, S., Yan, X., Zhao, Y., Li, B., and Sun, L. (2014) Selective binding and magnetic separation of histidine-tagged proteins using Ni^{2+}-decorated Fe_3O_4/hydroxyapatite composite nanoparticles. *Mater. Lett*. 126: 97-100.

[64] Kailasa, S.K. and Wu, H. (2010) Surface modified silver selinide nanoparticles as extracting probes to improve peptide/protein detection via nanoparticles-based liquid phase microextraction coupled with MALDI mass spectrometry. *Talanta*, 83: 527-534.

[65] Kailasa, S.K. and Wu, H. (2012) Dispersive liquid-liquid microextraction using functionalized $Mg(OH)_2$ NPs with oleic acid as hydrophobic affinity probes for the analysis of hydrophobic proteins in bacteria by MALDI MS. *Analyst*, 137: 4490-4496.

[66] Kailasa, S.K. and Wu, H. (2013) Surface modified $BaTiO_3$ nanoparticles as the matrix for phospholipids and as extracting probes for LLME of hydrophobic proteins in Escherichia coli by MALDI-MS. *Talanta*, 114: 283-290.

[67] Wen, Q., Wang, Y., Xu, K., Li, N., Zhang, H., Yang, Q., and Zhou, Y. (2016) Magnetic solid-phase extraction of protein by ionic liquid-coated Fe@graphene oxide. *Talanta*. 160: 481-488.

[68] Xu, K., Wang, Y., Ding, X., Huang, Y., Li, N., and Wen, Q. (2016) Magnetic solid-phase extraction of protein with deep eutectic solvent immobilized magnetic graphene oxide nanoparticles. *Talanta*, 148: 153-162.

[69] Huang, Y., Wang, Y., Wang, Y., Pan, Q., Ding, X., Xu, K., Li, N., and Wen, Q. (2016) Ionic liquid-coated Fe_3O_4/APTES/graphene oxide nanocomposites: synthesis, characterization and evaluation in protein extraction processes. *RSC Adv*., 6: 5718-5728.

[70] Tang, P., Cai, J., and Su, Q. (2009) Carbon nanotubes coated fiber for solid-phase microextraction of bovine fibrinogen and bovine serum albumin. J. *Chin. Chem. Soc*., 56: 1128-1138.

970 [71] Zhang, Y., Hu, Z., Qin, H., Wei, X., Cheng, K., Liu, F., Wu, R., and Zou, H. (2012) Highly
971 efficient extraction of cellular nucleic acid associated proteins in vitro with magnetic
972 oxidized carbon nanotubes. *Anal. Chem*., 84: 10454-10462.
973 [72] Quaresma, P., Osorio, I., Doria, G., Carvalho, P.A., Pereira, A., Langer, J., Araujo, J.P.,
974 Pastoriza-Santos, I., Liz-Marzan, L.M., Franco, R., Baptista, P.V., and Pereira, E. (2014)
975 Star-shaped magnetite@gold nanoparticles for protein magnetic separation and SERS
976 detection. *RSC Adv*. 4: 3659-3667.
977 [73] Daniele, M.A., Bandera, Y.P., Sharma, D., Rungta, P., Roeder, R., Sehorn, M.G., and
978 Foulger, S.H. (2012) Substrate-baited nanoparticles: A catch and release strategy for
979 enzyme recognition and harvesting. *Small,* 8: 2083-2090.
980 [74] Ye, N. (2008) Protein profiles of human serum by SELDI-TOF-MS with multiwalled
981 carbon nanotubes as absorbent. *Anal. Lett*., 41: 2554-2563.
982 [75] Du Z., Yu, Y., Chen, X., and Wang, J. (2007) The isolation of basic proteins by solid-phase
983 extraction with multiwalled carbon nanotubes. *Chem.-Eur. J*., 13: 9679-9685.
984 [76] Du, Z., Yu, Y., Yan, X., and Wang, J. (2008) Isolation and pre-concentration of basic
985 proteins in aqueous mixture via solid-phase extraction with multi-walled carbon nanotubes
986 assembled on a silica surface. *Analyst*, 133: 1373-1379.
987 [77] Du, Z., Yu, Y., and Wang, J. (2008) Selective isolation of acidic proteins with a thin layer
988 of multiwalled carbon nanotubes functionalized with polydiallyldimethylammonium
989 chloride. *Anal. Bioanal. Chem*., 392: 937-946.
990 [78] Li, Y., Lin, Y., Tsai, P., Chen, C., Chen, W., and Chen, Y. (2007) Nitrilotriacetic acid-
991 coated magnetic nanoparticles as affinity probes for enrichment of histidine-tagged
992 proteins and phosphorylated peptides. *Anal. Chem*., 79: 7519-7525.
993 [79] Sun, J., Rao, S., Su, Y., Xu, R., and Yang, Y. (2011) Magnetic carboxymethyl chitosan
994 nanoparticles with immobilized metal ions for lysozyme adsorption. *Colloid Surf. A-*
995 *Physicochem. Eng. Asp*., 389: 97-103.
996 [80] Dong, Y., Zhang, H., Yan, N., Zhou, L., Zhang, Z., Rahman, Z.U., and Chen, X. (2011)
997 Preparation of guanidine group functionalized magnetic nanoparticles and the application

998 in preconcentration and separation of acidic protein. *J. Nanosci. Nanotechnol*., 11: 10387-
999 10395.
1000 [81] Jian, G., Liu, Y., He, X., Chen, L., and Zhang, Y. (2012) Click chemistry: a new facile and
1001 efficient strategy for the preparation of Fe_3O_4 nanoparticles covalently functionalized with
1002 IDA-Cu and their application in the depletion of abundant protein in blood samples.
1003 *Nanoscale*, 4: 6336-6342.
1004 [82] Alwael, H., Connolly, D., Clarke, P., Thompson, R., Twamley, B., O'Connor, B., and Paull,
1005 B. (2011) Pipette-tip selective extraction of glycoproteins with lectin modified gold nano-
1006 particles on a polymer monolithic phase. *Analyst*, 136: 2619-2628.
1007 [83] Wang, A., Wu, C., and Chen, S. (2006) Gold nanoparticle-assisted protein enrichment and
1008 electroelution for biological samples containing low protein concentrations - A prelude of
1009 gel electrophoresis. *J. Proteome Res*., 5: 1488-1492.
1010 [84] Shastri, L., Kailasa, S.K., and Wu, H. (2010) Nanoparticle-single drop microextraction as
1011 multifunctional and sensitive nanoprobes: Binary matrix approach for gold nanoparticles
1012 modified with (4-mercaptophenyliminomethyl)-2-methoxyphenol for peptide and protein
1013 analysis in MALDI-TOF MS. *Talanta*, 81: 1176-1182.
1014 [85] Chiu, R.Y.T., Thach, A.V., Wu, C.M., Wu, B.M., and Kamei, D.T. (2015) An aqueous
1015 two-phase system for the concentration and extraction of proteins from the interface for
1016 detection using the lateral-flow immunoassay. *PLoS One*, 10, Article ID: e0142654.
1017 [86] Bhat, A.R. and Wu, H. (2010) Synthesis, characterization and application of modified Pd
1018 nanoparticles as preconcentration probes for selective enrichment/analysis of proteins via
1019 hydrophobic interactions from real-world samples using nanoparticle-liquid-liquid
1020 microextraction coupled to matrix-assisted laser desorption/ionization time-of-flight mass
1021 spectrometry. *Rapid Commun. Mass Spectrom*., 24: 3547-3552.
1022 [87] Wu, H., Kailasa, S.K., and Shastri, L. (2010) Electrostatically self-assembled azides on
1023 zinc sulfide nanoparticles as multifunctional nanoprobes for peptide and protein analysis
1024 in MALDI-TOF MS. *Talanta*, 82: 540-547.

[88] Shrivas, K. and Wu, H. (2012) Rapid and highly sensitive protein extraction via cobalt oxide nanoparticle-based liquid-liquid microextraction coupled with MALDI mass spectrometry. *Analyst*, 137: 890-895.

[89] Shrivas, K. and Wu, H. (2010) Multifunctional nanoparticles composite for MALDI-MS: Cd^{2+}-doped carbon nanotubes with CdS nanoparticles as the matrix, preconcentrating and accelerating probes of microwave enzymatic digestion of peptides and proteins for direct MALDI-MS analysis. *J. Mass Spectrom*., 45: 1452-1460.

[90] Xu, J., Yang, L., Han, Y., Wang, Y., Zhou, X., Gao, Z., Song, Y., and Schmuki, P. (2016) Carbon-decorated TiO2 nanotube membranes: A renewable nanofilter for charge-selective enrichment of proteins. *ACS Appl. Mater. Interfaces*, 8: 21997-22004.

[91] Liu, D., Yang, Q., Jin, S., Song, Y., Gao, J., Wang, Y., and Mi, H. (2014) Core-shell molecularly imprinted polymer nanoparticles with assistant recognition polymer chains for effective recognition and enrichment of natural low-abundance protein. *Acta Biomater*., 10: 769-775.

[92] Puzyr, A.P., Baron, A.V., Purtov, K.V., Bortnikov, E.V., Skobelev, N.N., Moginaya, O.A., and Bondar, V.S. (2007) Nanodiamonds with novel properties: A biological study. *Diam. Relat. Mat.,* 16: 2124-2128.

[93] Mubarak, N.M., Yusof, F., Alkhatib, M.F., Ameen, E., Khalid, M., Mohammed, A.S., Muataz, A., Qudsieh, I.Y., and Rashmi, W. (2010) Optimization of CNTs production using full factorial design and its advanced application in protein purification. *Int. J. Nanosci*., 9: 181-92.

[94] Mubarak, N.M., Yusof, F., and Alkhatib, M.F. (2011) The production of carbon nanotubes using two-stage chemical vapor deposition and their potential use in protein purification. *Chem. Eng. J.,* 168: 461-469.

[95] Okoli, C., Boutonnet, M., Mariey, L., Jaras, S., and Rajarao, G. (2011) Application of magnetic iron oxide nanoparticles prepared from microemulsions for protein purification. *J. Chem. Technol. Biotechnol*., 86: 1386-1393.

1052 [96] Okoli, C., Fornara, A., Qin, J., Toprak, M.S., Dalhammar, G., Muhammed, M., and
1053 Rajarao, G.K. (2011) Characterization of superparamagnetic iron oxide nanoparticles and
1054 its application in protein purification. *J. Nanosci. Nanotechnol*., 11: 10201-10206.
1055 [97] Ditsch, A., Yin, J., Laibinis, P.E., Wang, D.I.C., and Hatton, T.A. (2006) Ion-exchange
1056 purification of proteins using magnetic nanoclusters. *Biotechnol. Prog.*, 22: 1153-1162.
1057 [98] Gao, R., Mu, X., Zhang, J., and Tang, Y. (2014) Specific recognition of bovine serum
1058 albumin using superparamagnetic molecularly imprinted nanomaterials prepared by two-
1059 stage core-shell sol-gel polymerization, *J. Mat. Chem. B*, 2: 783-792.
1060 [99] Sun, S., Ma, M., Qiu, N., Huang, X., Cai, Z., Huang, Q., and Hu, X. (2011) Affinity
1061 adsorption and separation behaviors of avidin on biofunctional magnetic nanoparticles
1062 binding to iminobiotin. *Colloid Surf. B-Biointerfaces*, 88: 246-253.
1063 [100] Kose, K. and Denizli, A. (2013) Poly(hydroxyethyl methacrylate) based magnetic
1064 nanoparticles for lysozyme purification from chicken egg white. *Artif. Cell. Nanomed.*
1065 *Biotechnol*., 41: 13-20.
1066 [101] Zhu, X., Zhang, L., Fu, A., and Yuan, H. (2016) Efficient purification of lysozyme from
1067 egg white by 2-mercapto-5-benzimidazolesulfonic acid modified Fe_3O_4/Au nanoparticles.
1068 *Mater. Sci. Eng. C-Mater. Biol. Appl*., 59: 213-217.
1069 [102] Fan, J., Lu, J.G., Xu, R.S., Jiang, R., and Gao, Y. (2003) Use of water-dispersible Fe_2O_3
1070 nanoparticles with narrow size distributions in isolating avidin. J. *Colloid Interface Sci.*,
1071 266: 215-218.
1072 [103] Korhonen, H.J. and Rokka, S. (2012) Properties and applications of antimicrobial proteins
1073 and peptides from milk and eggs. In: Hettiarachchy, N.S. (Ed.), *Bioactive food proteins and*
1074 *peptides: Applications in human health*, CRC Press: Boca Raton, FL, USA. pp. 49-96.
1075 [104] Chang, S.Y., Zheng, N., Chen, C., Chen, C., Chen, Y., and Wang, C.R.C. (2007) Analysis
1076 of peptides and proteins affinity-bound to iron oxide nanoparticles by MALDI MS. *J. Am.*
1077 *Soc. Mass Spectrom*., 18: 910-918.

[105] Kim, H.M., Cho, E.J., and Bae, H. (2016) Single step purification of concanavalin A (Con A) and bio-sugar production from jack bean using glucosylated magnetic nano matrix. *Bioresour. Technol*., 213: 257-261.

[106] Lee, Y., Park, J., Huh, J., Kim, M., Lee, J., Palani, A., Lee, K., and Lee, S. (2010) Ultra-specific enrichment of GST-tagged protein by GSH-modified nanoparticles. *Bull. Korean Chem. Soc*., 31: 1568-1572.

[107] Wang, F., Guo, C., and Liu, C. (2013) Functional magnetic mesoporous nanoparticles for efficient purification of laccase from fermentation broth in magnetically stabilized fluidized bed, *Appl. Biochem. Biotechnol*., 171: 2165-2175.

[108] Nakamura-Tsuruta, S., Kishimoto, Y., Nishimura, T., and Suda, Y. (2008) One-step purification of lectins from banana pulp using sugar-immobilized gold nano-particles. *J. Biochem*., 143: 833-839.

[109] Vergara-Barberan, M., Jesús Lerma-García, M., Francisco Simó-Alfonso, E., and Manuel Herrero-Martínez, J. (2016) Solid-phase extraction based on ground methacrylate monolith modified with gold nanoparticles for isolation of proteins. *Anal. Chim. Acta*., 917: 37-43.

[110] Lundqvist, M., Berggård, T., Hellstrand, E., Lynch, I., Dawson, K.A., Linse, S., and Cedervall, T. (2011) Rapid and facile purification of apolipoprotein A-I from human plasma using thermoresponsive nanoparticles. *J. Biomater. Nanobiotechnol*., 2: 258-266.

[111] Bakry, R., Gjerde, D., and Bonn, G.K. (2006) Derivatized nanoparticle coated capillaries for purification and micro-extraction of proteins and peptides. *J. Proteome Res*., 5: 1321-1331.

[112] Bornhorst, J.A. and Falke, J.J. (2000) Purification of proteins using polyhistidine affinity tags. *Methods Enzymol.*, 326: 245-254.

[113] Porath, J., Carlsson, J., Olsson, I., and Belfrage, G. (1975) Metal chelate affinity chromatography, a new approach to protein fractionation. *Nature*, 258: 598-599.

[114] Walls, D. and Loughran, S.T. (2010) Tagging recombinant proteins to enhance solubility and aid purification. In: Walls, D., and Loughran, S.T. (Eds.), *Protein Chromatography: Methods and Protocols*, Humana Press: New York, NY, USA. pp. 151-175.

[115] Chen, Y., Jiang, P., Liu, S., Zhao, H., Cui, Y., and Qin, S. (2011) Purification of 6xHis-tagged phycobiliprotein using zinc-decorated silica-coated magnetic nanoparticles. *J. Chromatogr. B*, 879: 993-997.

[116] Block, H., Maertens, B., Spriestersbach, A., Brinker, N., Kubicek, J., Fabis, R., Labahn, J., and Schaefer, F. (2009) Immobilized-metal affinity chromatography (IMAC): A review, in: Guide to Protein Purification, second ed., *Methods Enzymol*. 463: 439-473.

[117] Mohapatra, S., Pal, D., Ghosh, S.K., and Pramanik, P. (2007) Design of superparamagnetic iron oxide nanoparticle for purification of recombinant proteins. *J. Nanosci. Nanotechnol*., 7: 3193-3199.

[118] Bloemen, M., Vanpraet, L., Ceulemans, M., Parac-Vogt, T.N., Clays, K., Geukens, N., Gils, A., and Verbiest, T. (2015) Selective protein purification by PEG-IDA-functionalized iron oxide nanoparticles. *RSC Adv*. 5: 66549-66553.

[119] Chiang, C., Chen, C., and Chang, L. (2008) Purification of recombinant enhanced green fluorescent protein expressed in Escherichia coli with new immobilized metal ion affinity magnetic absorbents. *J. Chromatogr. B*, 864: 116-122.

[120] Shieh, D., Su, C., Chang, F., Wu, Y., Su, W., Hwu, J.R., Chen, J., and Yeh, C. (2006) Aqueous nickel-nitrilotriacetate modified Fe_3O_4-NH_3^+ nanoparticles for protein purification and cell targeting. *Nanotechnology*, 17: 4174-4182.

[121] Sahu, S.K., Chakrabarty, A., Bhattacharya, D., Ghosh, S.K., and Pramanik, P. (2011) Single step surface modification of highly stable magnetic nanoparticles for purification of His-tag proteins. *J. Nanopart. Res*., 13: 2475-2484.

[122] Wang, W., Wang, D.I.C., and Li, Z. (2011) Facile fabrication of recyclable and active nanobiocatalyst: purification and immobilization of enzyme in one pot with Ni-NTA functionalized magnetic nanoparticle. *Chem. Commun*., 47: 8115-8117.

[123] Kim, J.S., Valencia, C.A., Liu, R., and Lin, W. (2007) Highly-efficient purification of native polyhistidine-tagged proteins by multivalent NTA-modified magnetic nanoparticles. *Bioconjug. Chem*., 18: 333-341.

1133 [124] Liao, Y., Cheng, Y., and Li, Q. (2007) Preparation of nitrilotriacetic acid/Co2+-linked,
1134 silicalboron-coated magnetite nanoparticles for purification of 6 x histidine-tagged
1135 proteins. *J. Chromatogr. A*, 1143: 65-71.
1136 [125] Fang, W., Chen, X., and Zheng, N. (2010) Superparamagnetic core-shell polymer particles
1137 for efficient purification of his-tagged proteins. *J. Mat. Chem*., 20: 8624-8630.
1138 [126] Tural, B., Sopaci, S.B., Ozkan, N., Demir, A.S., and Volkan, M. (2011) Preparation and
1139 characterization of surface modified gamma-Fe_2O_3 (maghemite)-silica nanocomposites
1140 used for the purification of benzaldehyde lyase. *J. Phys. Chem. Solids*., 72: 968-973.
1141 [127] Xu, F., Geiger, J.H., Baker, G.L., and Bruening, M.L. (2011) Polymer brush-modified
1142 magnetic nanoparticles for His-tagged protein purification. *Langmuir*, 27: 3106-3112.
1143 [128] Aygar, G., Kaya, M., Ozkan, N., Kocabiyik, S., and Volkan, M. (2015) Preparation of silica
1144 coated cobalt ferrite magnetic nanoparticles for the purification of histidine-tagged
1145 proteins. *J. Phys. Chem. Solids*., 87: 64-71.
1146 [129] Fraga García. P., Brammen. M., Wolf. M., Reinlein. S., von Roman. M.F., and
1147 Berensmeier, S. (2015) High-gradient magnetic separation for technical scale protein
1148 recovery using low cost magnetic nanoparticles. *Sep. Purif. Technol*., 150: 29-36.
1149 [130] Feng, G., Hu, D., Yang, L., Cui, Y., Cui, X., and Li, H. (2010) Immobilized-metal affinity
1150 chromatography adsorbent with paramagnetism and its application in purification of
1151 histidine-tagged proteins. *Sep. Purif. Technol*., 74: 253-260.
1152 [131] Cho, E.J., Kim, H.J., Song, Y., Choi, I.S., and Bae, H.-J. (2011) Phenanthroline-based
1153 magnetic nanoparticles as a general agent to bind Histidine-tagged proteins. *J. Nanosci.*
1154 *Nanotechnol*., 11: 7104-7107.
1155 [132] Cho, E.J., Jung, S., Lee, K., Lee, H.J., Nam, K.C., and Bae, H. (2010) Fluorescent receptor-
1156 immobilized silica-coated magnetic nanoparticles as a general binding agent for histidine-
1157 tagged proteins. *Chem. Commun*., 46: 6557-6559.
1158 [133] Yang, J., Ni, K., Wei, D., and Ren, Y. (2015) One-step purification and immobilization of
1159 his-tagged protein via Ni2+-functionalized Fe_3O_4@polydopamine magnetic nanoparticles.
1160 *Biotechnol. Bioprocess Eng*., 20: 901-907.

[134] Feczko, T., Muskotal, A., Gal, L., Szepvolgyi, J., Sebestyen, A., and Vonderviszt, F. (2008) Synthesis of Ni-Zn ferrite nanoparticles in radiofrequency thermal plasma reactor and their use for purification of histidine-tagged proteins. *J. Nanopart. Res*., 10: 227-232.

[135] Parisien, A., Al-Zarka, F., Hussack, G., Baranova, E.A., Thibault, J., and Lan, C.Q. (2012) Nickel nanoparticles synthesized by a modified polyol method for the purification of histidine-tagged single-domain antibody ToxA5.1. *J. Mater. Res*., 27: 2884-2890.

[136] Man-Hua, Z., Yan-Hui, W., Song, W., Shang-Wei, J., Yong-Gui, Z., Yan, L., Hong-Yan, L., and Jiang-Bin, W. (2011) C@Fe_3O_4/NTA-Ni magnetic nanospheres purify histidine-tagged fetidin: A technical note. *Afr. J. Biotechnol*., 10: 16602-16609.

[137] Zhang, L., Zhu, X., Jiao, D., Sun, Y., and Sun, H. (2013) Efficient purification of His-tagged protein by superparamagnetic Fe_3O_4/Au-ANTA-Co^{2+} nanoparticles. *Mater. Sci. Eng. C-Mater. Biol. Appl*., 33: 1989-1992.

[138] Li, X., Zhao, W., Gu, J., Li, Y., Li, L., Niu, D., and Shi, J. (2015) Facile synthesis of magnetic core-mesoporous shell structured sub-microspheres decorated with NiO nanoparticles for magnetic recyclable separation of proteins. *Microporous Mesoporous Mat*., 207: 142-148.

[139] Mirahmadi-Zare, S.Z., Allafchian, A., Aboutalebi, F., Shojaei, P., Khazaie, Y., Dormiani, K., Lachinani, L., and Nasr-Esfahani, M. (2016) Super magnetic nanoparticles $NiFe_2O_4$, coated with aluminum-nickel oxide sol-gel lattices to safe, sensitive and selective purification of his tagged proteins. *Protein Expr. Purif*., 121: 52-60.

[140] Okada, Y., Takano, T.Y., Kobayashi, N., Hayashi, A., Yonekura, M., Nishiyama, Y., Abe, T., Yoshida, T., Yamamoto, T.A., Seino, S., and Doi, T. (2011) New protein purification system using gold-magnetic beads and a novel peptide tag, "the methionine tag". *Bioconjug. Chem*., 22: 887-893.

[141] Rogers, J.C. and Bomgarden, R.D. (2016) Sample preparation for mass spectrometry-based proteomics; from proteomes to peptides. In: Mirzaei, H. and Carrasco, M. (Eds.), *Modern proteomics - Sample preparation, analysis and practical application (first ed.)*, Springer: Cham, Switzerland. pp. 43-62.

[142] González-García, E., Marina, M.L., and García, M.C. (2014) Plum (*Prunus Domestica* L.) by-product as a new and cheap source of bioactive peptides: Extraction method and peptides characterization. *J. Funct. Food*., 11: 428-437.

[143] González-García, E., Puchalska, P., Marina, M.L., and García, M.C. (2015) Fractionation and identification of antioxidant and angiotensin-converting enzyme-inhibitory peptides obtained from plum (*Prunus domestica* L.) stones. *J. Funct. Food*., 19: 376-384.

[144] García, M.C., Endermann, J., González-García, E., and Marina, M.L. (2015) HPLC-Q-TOF-MS identification of antioxidant and antihypertensive peptides recovered from cherry (*Prunus cerasus* L.) subproducts. J. *Agric. Food Chem*., 63: 1514-1520.

[145] Vásquez-Villanueva, R., Marina, M.L., and García, M.C. (2015) Revalorization of a peach (*Prunus persica* (L.) Batsch) byproduct: Extraction and characterization of ACE-inhibitory peptides from peach stones. *J. Funct. Food*., 18: 137-146.

[146] Vásquez-Villanueva, R., Marina, M.L., and García, M.C. (2016) Identification by hydrophilic interaction and reversed-phase liquid chromatography-tandem mass spectrometry of peptides with antioxidant capacity in food residues. *J. Chromatogr. A*, 1428: 185-192.

[147] Esteve, C., Marina, M.L., and García, M.C. (2015) Novel strategy for the revalorization of olive (*Olea europaea*) residues based on the extraction of bioactive peptides. *Food Chem*., 167: 272-280.

[148] Jun, S., Chang, M.S., Kim, B.C., An, H.J., Lopez-Ferrer, D., Zhao, R., Smith, R.D., Lee, S., and Kim, J. (2010) Trypsin coatings on electrospun and alcohol-dispersed polymer nanofibers for a trypsin digestion column. *Anal. Chem*., 82: 7828-7834.

[149] Datta, S., Christen, L.R., and Rajaram, Y.R.S. (2013) Enzyme immobilization: An overview on techniques and support materials. *3 Biotech*., 3: 1-9.

[150] Ju, S., and Yeo, W. (2012) Quantification of proteins on gold nanoparticles by combining MALDI-TOF MS and proteolysis. *Nanotechnology*, 23: 135701-135707.

[151] Seok, H.J., Hong, M.Y., Kim, Y.J., Han, M.K., Lee, D., Lee, J.H., Yoo, J.S., and Kim, H.S. (2005) Mass spectrometric analysis of affinity-captured proteins on a dendrimer-based

immunosensing surface: investigation of on-chip proteolytic digestion. *Anal. Biochem*., 337: 294-307.

[152] Pham, M.D., Yu, S.S.-F., Han, C., and Chan, S.I. (2013) Improved mass spectrometric analysis of membrane proteins based on rapid and versatile sample preparation on nanodiamond particles. *Anal. Chem*., 85: 6748-6755.

[153] Chen, W., and Chen, Y. (2007) Acceleration of microwave-assisted enzymatic digestion reactions by magnetite beads. *Anal. Chem*., 79: 2394-2401.

[154] Sharma, A. and Tapadia, K. (2016) Green tea-synthesized magnetic nanoparticles accelerate the microwave digestion of proteins analyzed by MALDI-TOF-MS. *J. Iran Chem. Soc*., 13: 1723-1732.

[155] Chen, W. and Chen, Y. (2010) Functional Fe_3O_4@ZnO magnetic nanoparticle-assisted enrichment and enzymatic digestion of phosphoproteins from saliva. *Anal. Bioanal. Chem.* 398: 2049-2057.

[156] Wu, H., Agrawal, K., Shrivas, K., and Lee, Y. (2010) On particle ionization/enrichment of multifunctional nanoprobes: washing/separation-free, acceleration and enrichment of microwave-assisted tryptic digestion of proteins via bare TiO_2 nanoparticles in ESI-MS and comparing to MALDI-MS. *J. Mass Spectrom*., 45: 1402-1408.

[157] Hasan. N., Wu. H., Li. Y., and Nawaz, M. (2010) Two-step on-particle ionization/enrichment via a washing- and separation-free approach: multifunctional TiO_2 nanoparticles as desalting, accelerating, and affinity probes for microwave-assisted tryptic digestion of phosphoproteins in ESI-MS and MALDI-MS: comparison with microscale TiO_2. *Anal. Bioanal. Chem*., 396: 2909-2919.

[158] Shrivas, K., Agrawal, K., and Wu, H. (2011) Application of platinum nanoparticles as affinity probe and matrix for direct analysis of small biomolecules and microwave digested proteins using matrix-assisted laser desorption/ionization mass spectrometry. *Analyst*, 136: 2852-2857.

[159] Chen, J., Hon, K., and Chen, Y. (2011) Multilayer gold nanoparticle-assisted protein tryptic digestion in solution and in gel under photothermal heating. *Anal. Bioanal. Chem*., 399: 377-385.

[160] Li, Y., Xu, X., Deng, C., Yang, P., and Zhang, X. (2007) Immobilization of trypsin on superparamagnetic nanoparticles for rapid and effective proteolysis. *J. Proteome Res*., 6: 3849-3855.

[161] Jeng, J., Lin, M., Cheng, F., Yeh, C., and Shiea, J. (2007) Using high-concentration trypsin-immobilized magnetic nanoparticles for rapid in situ protein digestion at elevated temperature. *Rapid Commun. Mass Spectrom*., 21: 3060-3068.

[162] Lin, S., Yun, D., Qi, D., Deng, C., Li, Y., and Zhang, X. (2008) Novel microwave-assisted digestion by trypsin-immobilized magnetic nanoparticles for proteomic analysis. *J. Proteome Res*., 7: 1297-1307.

[163] Miao, A., Dai, Y., Ji, Y., Jiang, Y., and Lu, Y. (2009) Liquid-chromatographic and mass-spectrometric identification of lens proteins using microwave-assisted digestion with trypsin-immobilized magnetic nanoparticles. *Biochem. Biophys. Res. Commun*., 380: 603-608.

[164] Li, Y., Wojcik, R., and Dovichi, N.J. (2011) A replaceable microreactor for on-line protein digestion in a two-dimensional capillary electrophoresis system with tandem mass spectrometry detection. *J. Chromatogr. A*, 1218: 2007-2011.

[165] Lee, B., López-Ferrer, D., Kim, B.C., Na, H.B., Park, Y.I., Weitz, K.K., Warner, M.G., Hyeon, T., Lee, S., Smith, R.D., and Kim, J. (2011) Rapid and efficient protein digestion using trypsin-coated magnetic nanoparticles under pressure cycles. *Proteomics*, 11: 309-318.

[166] Hu, Z., Zhao, L., Zhang, H., Zhang, Y., Wu, R., and Zou, H. (2014) The on-bead digestion of protein corona on nanoparticles by trypsin immobilized on the magnetic nanoparticle. *J. Chromatogr. A*, 1334: 55-63.

[167] Slovakova, M., Sedlak, M., Krizkova, B., Kupcik, R., Bulanek, R., Korecka, L., Drasar C., and Bilkova, Z. (2015) Application of trypsin Fe_3O_4@SiO_2 core/shell nanoparticles for protein digestion. *Process Biochem*., 50: 2088-2098.

[168] Qin, W., Song, Z., Fan, C., Zhang, W., Cai, Y., Zhang, Y., and Qian, X. (2012) Trypsin immobilization on hairy polymer chains hybrid magnetic nanoparticles for ultra fast, highly efficient proteome digestion, facile O-18 labeling and absolute protein quantification. *Anal. Chem*., 84: 3138-3144.

[169] Fan, C., Shi, Z., Pan, Y., Song, Z., Zhang, W., Zhao, X., Tian, F., Peng, B., Qin, W., Cai, Y., and Qian, X. (2014) Dual matrix-based immobilized trypsin for complementary proteolytic digestion and fast proteomics analysis with higher protein sequence coverage. *Anal. Chem*., 86: 1452-1458.

[170] Shen, Y., Guo, W., Qi, L., Qiao, J., Wang, F., and Mao, L. (2013) Immobilization of trypsin via reactive polymer grafting from magnetic nanoparticles for microwave-assisted digestion. *J. Mat. Chem. B*, 1: 2260-2267.

[171] Cheng, G. and Zheng, S. (2014) Construction of a high-performance magnetic enzyme nanosystem for rapid tryptic digestion. *Sci. Rep*., 4, Article ID: 6947.

[172] Lee, B., Kim, B.C., Chang, M.S., Kim, H.S., Na, H.B., Park, Y.I., Lee, J., Hyeon, T., Lee, H., Lee, S., and Kim, J. (2016) Efficient protein digestion using highly-stable and reproducible trypsin coatings on magnetic nanofibers. *Chem. Eng. J*., 288: 770-777.

[173] Duarte Neto, J.M.W., da Costa Maciel, J., Furtado Campos, J., de Carvalho Junior, L.B., Araújo Viana Marques, D., de Albuquerque Lima, C., and Figueiredo Porto, A.L. (2017) Optimization of *Penicillium aurantiogriseum* protease immobilization on magnetic nanoparticles for antioxidant peptides obtainment. *Prep. Biochem. Biotechnol*., 47: 644-654.

[174] Madadlou, A., Sheehan, D., Emam-Djomeh, Z., and Mousavi, M.E. (2011) Ultrasound-assisted generation of ACE-inhibitory peptides from casein hydrolyzed with nanoencapsulated protease. *J. Sci. Food Agric*., 91: 2112-2116.

1296 [175] Safdar, M., Spross, J., and Janis, J. (2013) Microscale enzyme reactors comprising gold
1297 nanoparticles with immobilized trypsin for efficient protein digestion. *J. Mass Spectrom.*,
1298 48: 1281-1284.
1299 [176] Gogoi, D., Barman, T., Choudhury, B., Khan, M., Chaudhari, Y., Dehingia, M., Pal, A.R.,
1300 Bailung, H., and Chutia, J. (2014) Immobilization of trypsin on plasma prepared Ag/PPAni
1301 nanocomposite film for efficient digestion of protein. *Mater. Sci. Eng. C-Mater. Biol. Appl.*,
1302 43: 237-242.
1303 [177] Höldrich, M., Sievers-Engler, A., and Laemmerhofer, M. (2016) Gold nanoparticle-
1304 conjugated pepsin for efficient solution-like heterogeneous biocatalysis in analytical
1305 sample preparation protocols. *Anal. Bioanal. Chem.*, 408: 5415-5427.
1306 [178] Wang, S., Bao, H., Yang, P., and Chen, G. (2008) Immobilization of trypsin in polyaniline-
1307 coated nano-Fe3O4/carbon nanotube composite for protein digestion. *Anal. Chim. Acta.*,
1308 612. 182-189.
1309 [179] Zhang, Y., Cao, W., Liu, M., Yang, S., Wu, H., Lu, H., and Yang, P. (2010) Immobilization
1310 of trypsin on water-soluble dendrimer-modified carbon nanotubes for on-plate proteolysis
1311 combined with MALDI-MS analysis. *Mol. Biosyst.*, 6: 1447-1449.
1312 [180] Jiang, B., Yang, K., Zhang, L., Liang, Z., Peng, X., and Zhang, Y. (2014) Dendrimer-
1313 grafted graphene oxide nanosheets as novel support for trypsin immobilization to achieve
1314 fast on-plate digestion of proteins. *Talanta*, 122: 278-284.
1315 [181] Huang, Y., Shan, W., Liu, B.H., Liu, Y., Zhang, Y.H., Zhao, Y., Lu, H.J., Tang, Y., and
1316 Yang, P.Y. (2006) Zeolite nanoparticle modified microchip reactor for efficient protein
1317 digestion. *Lab Chip.*, 6: 534-539.
1318 [182] Zhang, X., Wang, F., and Xia, Y. (2013) Trypsin functionalization and zirconia coating of
1319 mesoporous silica nanotubes for matrix-assisted laser desorption/ionization mass
1320 spectrometry analysis of phosphoprotein. *J. Chromatogr. A*, 1306: 20-26.
1321 [183] Sun, X., Cai, X., Wang, R., and Xiao, J. (2015) Immobilized trypsin on hydrophobic
1322 cellulose decorated nanoparticles shows good stability and reusability for protein digestion.
1323 *Anal. Biochem.*, 477: 21-27.

1324 **Table 1.** Revision works devoted to the evaluation of nanomaterials in different steps of protein sample preparation.

Nanomaterial	Application	Year	Reference
Nanomaterials	Liquid-phase microextraction with some applications to the extraction of proteins.	2015	[46]
	Micro-extraction techniques for the enrichment of biomolecules with some examples involving proteins.	2016	[47]
AuNPs	Sugar-immobilized AuNPs for protein purification.	2011	[48]
AuNPs-MNPs	AuNPs and AuNPs-MNPs composites for the extraction and enrichment of proteins	2012	[49]
MNPs	Biomedical applications with a short section devoted to proteins purification.	2009	[50]
	Proteins digestion and preconcentration.	2011	[51]
	Enzyme immobilization and protein purification related to food analysis applications.	2012	[52]
	Application in the biomedical field, including protein examples.	2016	[53]

1325

1326

1327 **Table 2.** Nanomaterials used in the extraction of proteins from real complex samples.
1328

Nanomaterial	Analyte	Sample	Type of interaction	Extraction time	Elution	LOD/ Detection technique	Adsorption capacity	Non-specific binding	Reuse	Ref.
CARBON-BASED NANOMATERIALS										
CNTs-IDA-Cu^{2+}	Minor proteins	Human serum	Chelate formation	1.5 h	Without elution	- (MELDI-TOF-MS)	-	-	-	[54]
MWCNTs–polyethyleneimine	BSA	Bovine serum	Electrostatic interaction	-	0.2 M NaCl	1 µg/mL (FIA-UV/Vis detection)	113 mg/g	-	At least 60 cycles	[55]
MAGNETIC METAL-BASED NANOMATERIALS										
γ-Fe_2O_3 - dsRNA [poly(IC)] NPs	35 kDa protein ((2-5)A synthetase)	*Lubomirskia baicalensis*	-	30 min	4 M urea (pH 7.0)	- (SDS-PAGE)	-	No	Yes	[56]
Fe_3O_4@DIH-EMIMLpro NPs	Hemoglobin	Human blood	Adsorption and electrostatic forces	15 min	Tris + SDS + NaCl	- (UV/Vis detection and SDS-PAGE)	1.58 mg/mg	Low for Lyz	At least 8 cycles	[57]
Fe_3O_4@SiO_2@ionic liquids NPs	Hemoglobin	Human blood	Complexation forces	~15 min	Na_2CO_3-$NaHCO_3$ buffer (pH = 10) + 0.5% (m/v) SDS	- (UV/Vis detection)	5.78 mg/mg	No	Yes	[58]
Fe_3O_4@MIP NPs	Lyz	Human urine	Protein-template interaction	2 h	Thermally modulated	- (UV/Vis detection)	204.1 mg/g	<10mg/g for pepsin, BSA, Cyto C, and Myo	At least 12 cycles	[60]
Fe_3O_4@hydroxyapatite-Ni^{2+} NPs	Histidine-tagged protein	*E. coli* cell lysate	Ni-histidine affinity	2 h	1.0 M imidazole	- (UV/Vis detection)	12.98 mmol/g	No	Capacity reduced in 20 % after 4 cycles	[63]
NON-MAGNETIC METAL-BASED NANOMATERIALS										
Ag_2Se@octadecanethiol and Ag_2Se@11-mercaptoundecanoic acid NPs	Hydrophobic proteins	Soybean	Hydrophobic interaction	1 h	Without elution	- (MALDI-TOF-MS)	-	-	-	[64]
$Mg(OH)_2$-oleic acid NPs	Hydrophobic proteins	Bacteria *E. coli* and *B. subtilis*	Hydrophobic interaction	45 min	Without elution	- (MALDI-TOF-MS)	-	-	-	[65]

Nanomaterial	Analyte	Sample	Type of interaction	Extraction time	Elution	LOD/ Detection technique	Adsorption capacity	Non-specific binding	Reuse	Ref.
$BaTiO_3$-HOA NPs	Hydrophobic proteins	*E. coli*	Hydrophobic interaction	30 min	Without elution	- (MALDI-TOF-MS)	-	-	-	[66]
NANOCOMPOSITES										
Fe NPs@GO@AFDCIL	Bovine hemoglobin	Porcine and bovine blood	H-bonds	1 h	4% SDS	11.87 µg/mL (UV/Vis detection)	174.54 mg/g	Low	At least 15 times	[67]
Fe_3O_4-NH_2@GO@DES NPs DES: ChCl-EG, ChCl-G, D-ChCl- Glu, D-ChCl-S	BSA and minor proteins	Bovine blood	H-bonds and electrostatic interaction	1 h	0.1 M Na_2HPO_4 + 1 M NaCl	13.74 µg/mL (UV/Vis detection)	10.02–44.59 mg/g	-	Loss of extraction capacity	[68]
Fe_3O_4@APTES@GO@IL NPs	BSA and minor proteins	Bovine calf blood	H-bonds, electrostatic and hydrophobic interactions	2 h	0.8 M K_2HPO_4 + 1 M NaCl	- (UV/Vis detection)	139.1 mg/g	-	-	[69]
PDMS fibers@SWCNTs and PDMS fibers@MWCNTs	BSA and BFg	Bovine plasma	Electrostatic interaction	2 – 2.5 h	3 M NaCl	BFg: 78 µg/mL (SDS-PAGE and fluorescence detection)	BFg: 2.2 mg	-	-	[70]
oMWCNT@Fe_3O_4	Nucleic acid associated proteins	Cell lysate	π-π stacking and hydrophobic interaction	1 min	Without elution	- (nLC-MS/MS)	109 ± 13 mg/g	Negligible for BSA	-	[71]
Fe_3O_4@AuNPs-NTA-Ni^{2+} NPs	Histidine-tagged maltose binding proteins	Cell lysate	Ni-histidine affinity	2 h	Phosphate buffer + 500 mM imidazole	- (SDS-PAGE)	-	No	-	[72]
OTHERS										
Poly(propargyl acrylate) - 9-(3-azidopropyl)-9H-carbazole NPs	CARDO proteins	*P. resinovorans* CA10 lysate	Enzyme-substrate interaction	1 h	500 mM imidazole	- (MALDI-TOF-MS and SDS-PAGE)	-	No	-	[73]

AFDCIL: amino functional dicationic ionic liquid; **APTES:** 3-aminopropyltriethoxysilane; **BFg:** bovine fibrinogen; **B. subtilis:** Bacillus subtilis; **CARDO:** carbazole 1-9 dioxygenase; **ChCl:** choline chloride; **CNTs:** carbon nanotubes; **DES:** deep eutectic solvent; **DIH-EMIMLpro:** 1, 6-diisocyanatohexan - 1-ethyl-3-methyl-imidazolium L-proline; **dsRNA:** double-stranded ribonucleic acid; **GO:** graphene oxide; **HOA:** 12-hydroxy octadecanoic acid; **IDA:** iminodiacetic acid; **IL:** ionic liquid; **MALDI-TOF-MS:** matrix-assisted laser desorption/ionization-time of flight-mass spectrometry; **MIP:** molecularly imprinted polymer; **MELDI-TOF-MS:** matrix-enhanced laser desorption/ionization-time of flight-mass spectrometry; **Myo:** myoglobin; **NTA:** nitriloacetic acid; **oMWCNTs:** oxidized multi-walled carbon nanotubes; **PDMS:** polydimethylsiloxane; **PEI:** polyethyleneimine.*Methods used for the extraction of standard proteins were not included.

1335 **Table 3.** Nanomaterials employed in the enrichment/(pre)concentration of proteins.

Nanomaterial	Analyte	Sample	Interaction	Time	Eluent	Enrich. factor	LOD/ Detection technique	Adsorpt. capacity	Reuse	Ref.
CARBON-BASED NANOMATERIALS										
MWCNTs	Proteins	Human serum	-	1 h	Without elution	10	- SELDI-TOF-MS	-	-	[74]
MWCNTs	Cyto C	Standard	Electrostatic interaction	-	0.5 M NaCl	15	0.06 µg/mL UV-Vis detection	24 mg/g	Yes, and at least 50 cycles without regeneration	[75]
MWCNTs	Hemoglobin	Standard and human whole blood	Electrostatic interaction	-	0.025 M PB (pH 8.0)	11	0.12 µg/mL UV-Vis detection	31 mg/g	Yes, and at least 50 cycles without regeneration	[75]
SiO_2@MWCNTs	Cyto C	Standard	Electrostatic interaction	-	0.5 M NaCl	30	0.02 µg/mL FIA-UV/Vis detection	112 mg/g	Yes	[76]
MWCNTs-PDDA	BSA	Standard	Electrostatic interaction	-	0.04 M citrate buffer	17	1.0 µg/mL FIA-UV/Vis detection	3800 mg/g	40-100 cycles (depending of the flow rate)	[77]
MWCNTs-PDDA	HSA	Blood	Electrostatic interaction	-	0.04 M citrate buffer	-	-	-	40-100 cycles (depending of the flow rate)	[77]
MAGNETIC METAL-BASED NANOMATERIALS										
Fe_3O_4 – NTA-Ni^{2+} NPs	6xHis-tag mutated streptopain	*E. coli* cell lysate	Ni-histidine affinity	30 s	Without elution	-	- (MALDI-MS)	200 mg/g	-	[78]
Fe_3O_4@(PEG+CM-CTS)@Zn^{2+}, Fe_3O_4@(PEG+CM-CTS)@Cu^{2+}, and Fe_3O_4@(PEG+CM-CTS)@Fe^{2+} NPs	Lyz	Standard	Metal ions-proteins affinity	1 h	0.2 M imidazole (pH 8.0) + 0.2 M NaCl	-	- Fluoresc.	Zn: 200 mg/g Cu: 185.19 mg/g Fe: 232.56 mg/g	No more than 2 or 3 cycles	[79]
Fe_3O_4@SiO_2@NH_2 – guanidine NPs	BSA	Standard	H-bond and electrostatic interaction	20 min	10 mM NaH_2PO_4 solution (pH 3.0)	15	45 ng/mL CE	10.7 mg/g	-	[80]
Fe_3O_4@SiO_2 – IDA-Cu^{2+} NPs	Hemoglobin	Bovine and human blood	Metal ion protein affinity	6 h	0.1 g/mL imidazole	-	- UV/Vis detection	38.2 mg/g	At least 5 cycles	[81]

Nanomaterial	Analyte	Sample	Interaction	Time	Eluent	Enrich. factor	LOD/ Detection technique	Adsorpt. capacity	Reuse	Ref.
NON-MAGNETIC METAL-BASED NANOMATERIALS										
AuNPs-*Erythrina cristagalli* lectin	Galactosylated protein (desialylated transferrin)	Standard	-	-	0.8 M galactose (40 µL)	-	- Capillary LC-UV/Vis	-	Yes	[82]
AuNPs-*Erythrina cristagalli* lectin	Galactosylated glycoproteins	*E. coli* cell lysate	Lectin-glycoprotein affinity	-	0.8 M galactose (40 µL)	-	- Capillary LC-UV/Vis	-	Yes	[82]
AuNPs	BSA and β-casein	Standards	-	-	Without elution	5	- nHPLC-Q-TOF-MS/MS	-	-	[83]
AuNPs	Proteins	Human urine	-	-	Without elution	5	- nHPLC-Q-TOF-MS/MS	-	-	[83]
AuNPs – (4-mercaptophenyliminomethyl)-2-methoxyphenol	Insulin, ubiquitin, Cyto C, Lyz, and Myo	Standards	Affinity interaction	1 h	Direct detection	-	fmol MALDI-TOF-MS	-	-	[84]
AuNPs – (4-mercaptophenyliminomethyl)-2-methoxyphenol	Lyz	Milk	Affinity interaction	1 h	Direct detection	-	fmol MALDI-TOF-MS	-	-	[84]
AuNPs – transferrin anti-body	Transferrin	Standard Fetal bovine serum and synthetic urine	Antigen-antibody interaction	10 min	Direct detection	-	0.01 ng/µL Lateral-flow immunoassay	-	-	[85]
Pd – octadecanethiol NPs	Lyz	Milk	Hydrophobic interaction	1 h	Without elution	-	- MALDI-TOF-MS	-	-	[86]
Pd – octadecanethiol NPs	Ubiquitin	Mushrooms and soybean	Hydrophobic interaction	1 h	Without elution	-	- MALDI-TOF-MS	-	-	[86]
Pd – octadecanethiol NPs	Insulin	Standard, rat pancreas, and urine	Hydrophobic interaction	1 h	Without elution	-	Insulin: 37 nM (urine) MALDI-TOF-MS	-	-	[86]
ZnS-N_3 NPs	Insulin, ubiquitin, Cyto C, Lyz, Myo, and BSA	Standards	Electrostatic interaction	1 h	Without elution	2-10	- MALDI-TOF-MS	-	-	[87]
ZnS-N_3 NPs	Proteins	Milk	Electrostatic interaction	1 h	Without elution	2-10	- MALDI-TOF-MS	-	-	[87]

Nanomaterial	Analyte	Sample	Interaction	Time	Eluent	Enrich. factor	LOD/ Detection technique	Adsorpt. capacity	Reuse	Ref.
ZnS-N_3 NPs	Ubiquitin and ubiquitin like proteins	Oyster mushroom	Electrostatic interaction	1 h	Without elution	2-10	- MALDI-TOF-MS	-	-	[87]
Co_3O_4 – CTA^+ NPs	Insulin and chymotrypsinogen	Standard	Electrostatic interaction	10 min	Without elution	Insulin: 12.5	Insulin: 5 nM MALDI-TOF-MS	-	-	[88]
Co_3O_4 – CTA^+ NPs	Lyz	Cow's milk	Electrostatic interaction	10 min	Without elution	4	- MALDI-TOF-MS	-	-	[88]
DENDRIMERS										
Carboxylate-terminated carbosilane dendrimers	BSA, Lyz, and Myo	Standards	Electrostatic interaction	30 min	0.1% SDS or heating 50 ^{0}C	-	- Bradford	-	-	[40]
Carboxylate-terminated carbosilane dendrimers	Proteins	Plum seeds	Electrostatic interaction	30 min	0.1% SDS or heating 50 ^{0}C	-	- Bradford	-	-	[40]
NANOCOMPOSITES										
MWCNT@CdS@Cd^{2+}	Ubiquitin	Standard	Electrostatic interaction	15 min	Direct analysis	12	- MALDI-TOF-MS	-	-	[89]
TiO_2@C nanotube membranes	HSA	Human blood	Hydrophobic interaction	-	Briton-Robinson buffer (pH 8.8)	-	- Bradford	41.8 mg/g	Up to 5 cycles	[90]
SiO_2@ARPCs-MIP NPs	Immunoglobulin heavy chain binding protein from endoplasmic reticulum	Pig liver	Protein-template interaction	8 h	500 mM KCl + 20 mM Na_2HPO_4/ NaH_2PO_4, pH 7.3	116	- BCA method	5.4 µg/g	-	[91]

ARPCs: assistant recognition polymer chains; **BCA:** bicinchoninic acid; **CE:** capillary electrophoresis; **CM-CTS:** carboxymethyl chitosan; **CTA:** cetyltrimethylammonium; ***E. coli*:** *Escherichia coli*; **FIA:** flow injection analysis; **HSA:** human serum albumin; **IDA:** iminodiacetic acid; **MALDI-TOF-MS:** matrix-assisted laser desorption/ionization-time of flight-mass spectrometry; **MIP:** molecularly imprinted polymer; **Myo:** myoglobin; **nHPLC-Q-TOF-MS:** nano high performance liquid chromatography-quadrupole-time of flight-mass spectrometry; **NTA:** nitriloacetic acid; **PB:** phosphate buffer; **PDDA:** poly(diallyldimethylammonium chloride); **PEG:** polyethylene glycol; **SELDI:** surface-enhanced laser desorption/ionization.

1341 **Table 4.** Nanomaterials employed in the purification of proteins by nanomaterial-based methods.
1342

Nanomaterial	Analyte	Sample	Interaction	Time	Eluent	Purification efficiency	Adsorpt. Capacity (mg/g)	Reuse	Ref.
NON-HISTIDINE-TAGGED PROTEINS PURIFICATION									
CARBON-BASED NANOMATERIALS									
NDs (RUDD) and modified NDs (RUDDM)	Catalase, histone fraction, and Lyz	Proteins standards	-	1 min	-	-	-	-	[92]
CNTs (acidic treatment)	Protein	Skim latex serum	Ion exchange interaction	-	2 M ammonium sulphate	-	-	-	[93,94]
MAGNETIC METAL-BASED NANOMATERIALS									
ME-MIONs (Fe_3O_4 - γ-Fe_2O_3) SPIONs (Fe_3O_4 - γ-Fe_2O_3)	Coagulant protein	*Moringa oleifera* seeds	Electrostatic interaction	1 h	0.8 M NaCl	Protein activity: ME-MIONs: 90% SPIONs: 84%	ME-MIONs: 400 SPIONs: 450	Yes	[95]
Fe_3O_4@trisodium citrate and Fe_3O_4 @SiO_2 NPs	Coagulant protein	*Moringa oleifera* seeds	Electrostatic interaction	30 min	0.8 M NaCl	Protein activity: Trisodium: 80% SiO_2: Low	-	-	[96]
Polymer-coated magnetic nanoclusters (Fe_3O_4)	Cyto C, BSA, and Lyz	Protein standards	Electrostatic and hydrophobic interactions	-	0.5 M NaCl	-	Cyto C: 640	Yes	[97]
Polymer-coated magnetic nanoclusters (Fe_3O_4)	Drosomycin	Cell-free *Pichia pastoris* fermentation broth	Electrostatic and hydrophobic interactions	-	50 mM TES	Purity: 90%	30	Yes	[97]
Fe_3O_4@MIPs–BSA NPs	BSA	Bovine blood	Electrostatic interaction and imprinted recognition	15 min	0.1 M NaOH	-	37.58	At least 10 cycles	[98]
Fe_3O_4-iminobiotin NPs	Avidin	Egg White	Avidin-iminobiotin affinitiy	45 min	0.1 M ammonium acetate (pH4.0) + 0.5 M NaCl	Purity: 98.5% Recovery: 92.8%	225	No more than 2 cycles	[99]
Fe_3O_4@PHEMATrp NPs	Lyz	Proteins standard and chicken egg white	Hydrophobic interaction	2 h	50 % ethylene glycol	Purity: 92 % Recovery: 76%	385.2	Up to 5 cycles	[100]
Fe_3O_4@Au-MBISA NPs	Lyz	Protein standard and egg white	Electrostatic interaction	20 min	20 mM PB (pH 8.0) + 1 M NaCl	-	346	Above 90 % after 7 cycles	[101]

Nanomaterial	Analyte	Sample	Interaction	Time	Eluent	Purification efficiency	Adsorpt. Capacity (mg/g)	Reuse	Ref.
Fe_3O_4 – oleate NPs	Insulin, Myo and Cyto C	Standards	Electrostatic and hydrophobic interactions	1 h	Without elution	-	Insulin: 323 Myo: 818	-	[104]
Fe_3O_4@SiO_2 – gluocosylated derivate 2 NPs	Concanavalin A	Jack bean	Gluocose-Concanavalin A (lectin) binding	5 min	0.1 M H_3PO_4	-	-	Yes	[105]
Fe_3O_4@SiO_2 – GSH NPs	GST-tag ubiquitin	Proteins standard, yeast enolase and human serum	Enzyme-substrate interactions	10 min	Without elution	-	-	-	[106]
Fe_3O_4@SiO_2-Cu^{2+} NPs	Laccase	Fermentation broth of *Trametes versicolor*	Metal affinity adsorption and size selectivity	-	20 mM PB + 200 mM imidazole	Purification fold: 62.4 Activity yield: 108.9%	192.5	At least 6 cycles	[107]
NON-MAGNETIC METAL-BASED NANOMATERIALS									
AuNPs–Sugar	Lectins	Banana pulp	Sugar-lectin affinity	Overnight	Inhibitory sugar	-	-	-	[108]
AuNPs – GMA-co-EDMA	BSA and Cyto C	Protein standards	Hydrophobic and electrostatic interactions	-	pH-controlled	Recovery: 95-98%	BSA: 16.6	-	[109]
AuNPs – GMA-co-EDMA	Lectins	European mistletoe leaves	Hydrophobic and electrostatic interactions	-	pH-controlled	-	-	-	[109]
OTHERS									
NIPAM:BAM copolymer NPs	Apolipoprotein A-I	Human plasma	Copolymer-apolipoprotein affinity	1 h	1) 6 M urea +10 mM Tris/HCl (pH 7.5) + 1 mM EDTA 2) Ion exchange chromatography	Purification efficiency: 13%	13	-	[110]
Concanavalin A-polystyrene latex NPs-capillary	Glycoprotein (ovalbumin)	Protein standard	Concanavalin A (lectin)-glycoprotein affinity	-	0.5 M methyl-R-mannopyranoside	-	-	-	[111]
Protein G-polystyrene latex NPs-capillary	Bovine immunoglobulin	Protein standard	Protein G-immunoglobulin affinity	-	10 mM HCl pH 2.5	-	-	-	[111]
HISTIDINE-TAGGED PROTEINS PURIFICATION									
MAGNETIC METAL-BASED NANOMATERIALS									
Fe_3O_4@SiO_2 – Zn^{2+} NPs	6xHis-tag recombinant phycobiliproteins	*E. coli* lysate	Zn^{2+}-histidine affinity interaction	30 min	10 mM PB + 500 mM imidazole (pH 7.4)	Recovery: 83%	923-1200	-	[115]

Nanomaterial	Analyte	Sample	Interaction	Time	Eluent	Purification efficiency	Adsorpt. Capacity (mg/g)	Reuse	Ref.
Fe_3O_4@SiO_2-IDA-Ni^{2+} NPs	6xHis-tag recombinant nitroreductase	*E. coli*	Ni^{2+}-histidine affinity interaction	30 min	200 mM imidazole	-	1500	Yes	[117]
Fe_3O_4–IDA-PEG-Ni^{2+} NPs	His-tag fluorescent *Discosoma sp*. red proteins	Cell lysate	Ni^{2+}-histidine affinity interaction	-	0.5 M imidazole	-	-	-	[118]
Fe_3O_4@GMA – IDA-Cu^{2+}-, Ni^{2+}-, and Zn^{2+} NPs	His-tag recombinant EGFP	*E. coli*	Metal ion-histidine affinity interaction	10 min	0.5 M imidazole	Recovery/ purification factor: Cu^{2+}: 70.4%/12.3 Ni^{2+}: 66.2%/7.6 Zn^{2+}: 63.7%/8.8	53.5	Yes	[119]
Fe_3O_4 – NTA-Ni^{2+} NPs	6xHis-tag streptopain	*E. coli* crude cell lysate	Ni^{2+}-histidine affinity interaction	20 min	400 mM imidazole	-	230	Yes	[120]
Fe_3O_4 – NTA-Ni^{2+} NPs	6xHis-tag recombinant protein (Malic enzyme)	*E. coli* cell lysate	Ni^{2+}-histidine affinity interaction	1 h	50 mM PB + 100 mM NaCl + 200 mM imidazole	-	-	Yes	[121]
Fe_3O_4 – NTA-Ni^{2+} NPs	His-tag enzyme (Solanum tuberosum epoxide hydrolase)	*Pichia pastoris* cell extract	Ni^{2+}-histidine affinity interaction	12 h	Imidazole	-	146	Capacity reduced in 20 % after 8 cycles	[122]
Fe_3O_4 – Bis- NTA-Ni^{2+} NPs	6xHis-tag recombinant mouse endostatin	*E. coli*	Ni^{2+}-histidine affinity interaction	1 h	50 mM PB + 300 mM NaCl + 250 mM imidazole (pH 8.0)	-	61.3	Yes	[123]
Fe_3O_4@(SiO_2+B_2O_3) – NTA-Co^{2+} NPs	6xHis-tag recombinant proteins	Bacterial cell lysate	Co^{2+}-histidine affinity interaction	30 min	50 mM NaH_2PO_4 + 300 mM NaCl + 250 mM imidazole + 0.05% Tween 20 (pH 8.0)	-	1.55	Loss of 60% capacity	[124]
Fe_3O_4@SiO_2-poly(styrene-alt-maleic anhydride)–NTA-Ni^{2+} NPs	His-tag GFP	*E. coli*	Ni^{2+}-histidine affinity interaction	10 min	500 mM imidazole	Recovery: 77%	-	Capacity reduced in 20 % after 5 cycles	[125]

Nanomaterial	Analyte	Sample	Interaction	Time	Eluent	Purification efficiency	Adsorpt. Capacity (mg/g)	Reuse	Ref.
SiO_2@γ-Fe_2O_3 - GPTMS-NTA-Co^{2+} NPs	His-tag recombinant benzaldehyde lyase (BAL, EC 4.1.2.38)	*E. coli* crude extract	Co^{2+}-histidine affinity interaction	-	PB + 200 mM imidazole	-	3.16 ± 0.4	At least 3 cycles	[126]
Fe_3O_4@SiO_2-PHEMA-SA-NTA-Cu^{2+} and Ni^{2+} NPs	His-tag cellular retinaldehyde-binding protein	Cell lysate	Ni^{2+}-histidine affinity interaction	5 min	20 mM PB (pH 7.2) + 0.5 M NaCl + 0.5 M imidazol	-	-	Yes	[127]
$CoFe_2O_4$@SiO_2-NTA-Ni^{2+} NPs	6xHis-tag heat shock protein (Tpv-sHSP 14.3)	*Thermoplasma volcanium*	Ni^{2+}-histidine affinity interaction	1 h	PB + 250 mM imidazole	-	-	-	[128]
Fe_3O_4@SiO_2-EDTA-Cu^{2+}	His-tag GFP	*E. coli* cell lysate	Cu^{2+}-histidine affinity interaction	25 min	0.05 M NaH_2PO_4 + 0.05 M imidazole + 0.5 M NaCl (pH = 7.9)	Purity: 96% Recovery: 93%	-	Yes	[129]
Fe_3O_4@SiO_2-GPTMS-aspartic acid-Co^{2+} NPs	6xHis-tag recombinant gp41 proteins	*E. coli* cell lysate	Co^{2+}-histidine affinity interaction	1 h	50 mM NaH_2PO_4 + 300 mM NaCl + 250 mM imidazole (pH 8.0)	-	9.45	-	[130]
Fe_3O_4@SiO_2-phenantroline-Cu^{2+} NPs	His-tag Cel5C protein	Cell lysate	Cu^{2+}-histidine affinity interaction	5 min	50, 250, and 500 mM imidazole	Purification fold: 0.99 Activity yield: 100%	-	Yes	[131]
Fe_3O_4@SiO_2-terpyridine receptor-Cu^{2+} NPs	His-tag GST, β-glucosidase and Cel5A proteins	Protein standards	Cu^{2+}-histidine affinity interaction	-	Imidazole	Purification fold: 1.11 Activity yield: 99.78%	-	Yes	[132]
Fe_3O_4–polydopamine-Ni^{2+} NPs	His-tag red fluorescent protein	Protein standards	Ni^{2+}-histidine affinity interaction	5 min	PBS + 300 mM imidazole	-	-	Yes	[133]
Ni-Zn Fe_2O_4 NPs	6xHis-tag FliJ from Salmonella typhimurium and TEV protease	*E. coli*	-	30 min	20 mM Na_2HPO_4 + 500 mM NaCl + imidazole (pH 7.4)	-	70	-	[134]
NON-MAGNETIC METAL-BASED NANOMATERIALS									
Ni NPs	6xHis-tag recombinant protein (ToxA5.1)	*E. coli*	Ni-histidine affinity interaction	2 min	100 mM HEPES + 500 mM imidazoles (pH 7.5)	-	-	4 cycles	[135]
NANOCOMPOSITES									
Fe_3O_4@AuNPs – NTA-Ni^{2+} NPs	His-tag maltose binding proteins	Cell lysate	Ni^{2+}-histidine affinity interaction	2 h	PB + 500 mM imidazole	-	-	-	[72]

Nanomaterial	Analyte	Sample	Interaction	Time	Eluent	Purification efficiency	Adsorpt. Capacity (mg/g)	Reuse	Ref.
C@Fe_3O_4 – NTA-Ni^{2+} NPs	6xHis-tag fetidin	*E. coli* lysate	Ni^{2+}-histidine affinity interaction	2 h	50 mM NaH_2PO_4 + 300 mM NaCl + 250 mM imidazole (pH 8.0)	Recovery: 20.94%	210.3	-	[136]
Fe_3O_4@ Au – ANTA-Co^{2+} NPs	His-tag proteins	*E. coli* lysate	Co^{2+}-histidine affinity interaction	10 min	50 mM NaH_2PO_4 + 300 mM NaCl + 250 mM imidazole	-	74	4 cycles above 80 % and then decrease	[137]
Fe_2O_3@SiO_2 – NiO NPs	His-tag GFP	Protein standard	Ni^{2+}-histidine affinity interaction	10 min	0.1 g/mL imidazole	-	-	At least 5 cycles	[138]
Fe_2O_3@SiO_2 – NiO NPs	His-tag proteins	*E. coli* cell lysate	Affinity interaction	10 min	0.1 g/mL imidazole	-	-	At least 5 cycles	[138]
$NiFe_2O_4$@$NiAl_2O_4$NPs	His-tag hIGF-1, GM-CSF and bFGF recombinant proteins	*E. coli*	-	30 min	50 mM $NaHPO_4$ + 300 mM NaCl + 250 mM imidazole (pH 8.00)	-	hIGF-1: 248 ± 84	At least 20 cycles	[139]
Fe_3O_4@AuNPs – phosphorylcholine NPs	Met-tag and Met- and Gly-tag EGFP	*E. coli* crude extract	Affinity interaction	30 min	20 mM Tris-HCl (pH 8.0) + 100 mM NaCl + 24 mM 2-ME	-	-	-	[140]
OTHERS									
Capillary - polystyrene latex – IDA-Ni^{2+} NPs	His-tag protein (6xHis-MP1 from whole lysate)	Protein standard	Ni^{2+}-histidine affinity interaction	-	Without elution	-	-	-	[111]

ANTA: Nα,Nα-bis(carboxymethyl)-L-lysine hydrate; **bFGF:** basic fibroblast growth factor; **CNT:** carbon nanotubes; **EDTA:** ethylene diamine tetraacetic acid; **(E)GFP:** (enhanced) green fluorescent protein; **Gly-tag:** glycine-tagged; **GMA-co-EDMA:** glycidyl methacrylate-co-ethylene dimethacrylate; **GM-CSF:** granulocyte-macrophage colony-stimulating factor; **GPTMS:** 3-glycidoxy propyltrimethoxy silane; **GSH:** Glutathione; **GST:** glutathione S-transferase; **HEPES:** 4-(2-hydroxyethyl)-1-piperazineethanesulfonic acid; **hIGF-1:** human insulin growth factor I; **IDA:** iminodiacetic acid; **MBISA:** 2-mercapto-5-benzimidazolesulfonic acid; **ME-MIONs:** microemulsion magnetic iron oxide nanoparticles; **Met-tag:** methionine-tagged; **MIP:** molecularly imprinted polymer; **Myo:** myoglobin; **ND:** nanodiamonds; **NIPAM:BAM:** N-isopropylacrylamide-N-tert-butylacrylamide; **NTA:** nitriloacetic acid; **PB:** phosphate buffer; **PEG:** polyethylene glycol; **PHEMA:** poly(2-hydroxyethyl methacrylate); **PHEMATrp:** poly(hydroxyethyl methacrylate-N-methacryloyl-(L)-tryptophan); **SA:** succinic anhydride; **SPIONs:** superparamagnetic iron oxide nanoparticles; **TES:** N-tris(hydroxymethyl)-methyl-2-aminoethanesulfonic acid; **TEV:** Tobacco Etch Virus.

1353 **Table 5.** Nanomaterials employed in the protein digestion, either as support or functionalized with an enzyme.

Nanomaterial	Type of digestion	Digestion time	Analyte	Sample	Sequence coverage (%)	Peptide matched	Peptides with missed cleavages	Reuse	Ref.
NANOMATERIALS USED TO SUPPORT PROTEINS FOR THEIR DIGESTION									
ON-BEAD DIGESTION									
Fe_3O_4-oleate NPs	On-bead tryptic digestion	24 h	Cyto C	Protein standards	-	12	9	-	[104]
oMWCNT@Fe_3O_4 NPs	On-bead tryptic digestion	16 h	Nucleic acid associated proteins	Cell lysate	-	-	-	-	[71]
AuNPs	On-bead tryptic digestion	6 h	BSA	Protein standard	-	-	-	-	[150]
PAMAM dendrimer (G4)	On-chip tryptic digestion	3 h	BSA, Lyz, and ferritin	Protein standards	BSA: 16 Lyz: 33 Ferritin: 33	BSA: 12 Lyz: 4 Ferritin: 6	BSA:3	-	[151]
PAMAM dendrimer (G4)	On-chip tryptic digestion	3 h	BSA	Human serum	16	10	-	-	[151]
PAMAM dendrimer (G4)	On-chip tryptic digestion	3 h	Proteins	*E. coli*	27-33	-	-	-	[151]
Surface-oxidized NDs	On-bead tryptic digestion	5 min	Particulate methane monooxygenase and membrane proteins	*E. coli*	23-50	-	-	-	[152]
MW-ASSISTED DIGESTION									
Fe_3O_4 NPs	MW-assisted tryptic digestion	30s-1min	Cyto C and Myo	Protein standards	Cyto C: 89 Myo: 90	Cyto C: 23 Myo:19	Cyto C: 21 Myo: 17	-	[153]
Fe_3O_4-NTA-Ni^{2+} NPs	MW-assisted tryptic digestion	2 min	6xHis-tag mutated streptopain	*E. coli* cell lysate	68.2	13	-	-	[78]
Fe_3O_4@SiO_2-APTES NPs	MW-assisted tryptic digestion	40 s	Cyto C	Protein standard	100	23	-	-	[154]
Fe_3O_4@ZnO NPs	MW-assisted tryptic digestion	1 min	Phosphoproteins	Human saliva	-	8	-	-	[155]
TiO_2 NPs	MW-assisted tryptic digestion	40-60 s	Cyto C, Lyz and Myo	Protein standards	Cyto C:100	Cyto C: 21	-	-	[156]

Nanomaterial	Type of digestion	Digestion time	Analyte	Sample	Sequence coverage (%)	Peptide matched	Peptides with missed cleavages	Reuse	Ref.
TiO_2 NPs	MW-assisted tryptic digestion	45 s	α- and β-casein	Protein standards	-	α-casein:12 β-casein:4	α-casein:5 β-casein:2	-	[157]
TiO_2 NPs	MW-assisted tryptic digestion	45 s	Phosphoproteins	Milk	-	-	-	-	[157]
ZnS-N_3 NPs	MW-assisted tryptic digestion	30-50 s	Cyto C and Lyz	Protein standards	-	Cyto C: 11 Lyz: 9	Cyto C:6 Lyz:3	-	[87]
Pt NPs	MW-assisted tryptic digestion	1 min	Lyz and BSA	Protein standards	-	-	-	-	[158]
MWCNT@CdS@Cd^{2+} NPs	MW-assisted tryptic digestion	1 min	Cyto C	Protein standard	-	15	-	-	[89]
MWCNT@CdS@Cd^{2+} NPs	MW-assisted tryptic digestion	1 min	Lyz	Cow milk	-	7	-	-	[89]
NIR-ASSISTED DIGESTION									
Glass@AuNPs	NIR-assisted in-solution tryptic digestion	3.5 min	Cyto C, Myo, BSA, and IgG	Protein standards	Cyto C: 95	Cyto C: 23	Cyto C: 19	Yes	[159]
Glass@AuNPs	NIR-assisted in-gel tryptic digestion	< 5 min	Cyto C, Myo, BSA, and IgG	Protein standards	BSA:12	BSA: 23	BSA: 16	Yes	[159]
Glass@AuNPs	NIR-assisted in-gel tryptic digestion	5 min	Proteins (HSA)	Human serum	35	22	18	Yes	[159]
NANOMATERIALS USED FOR THE IMMOBILIZATION OF ENZYMES									
MAGNETIC METAL-BASED NANOMATERIALS									
Fe_3O_4-trypsin NPs	Tryptic digestion	5 min	Cyto C, BSA, and Myo	Protein standards	Cyto C: 76 BSA: 46 Myo: 90	Cyto C:13 BSA: 30 Myo: 15	Cyto C: 8 BSA:13 Myo: 7	< 9 cycles	[160]
Fe_3O_4-trypsin NPs	Elevated temperature tryptic digestion	1 min	Cyto C, Myo, and Lyz	Protein standards	Cyto C: 49 Myo: 32 Lyz:57	Cyto C:10 Myo: 7 Lyz:11	-	< 9 cycles	[161]
Fe_3O_4-trypsin NPs	Tryptic digestion	3 h	IgG	Protein standard	21	2	-	< 9 cycles	[161]
Fe_3O_4-trypsin NPs	Tryptic digestion	3 h	HSA	Human serum	29	17	-	< 9 cycles	[161]
Fe_3O_4-trypsin NPs	MW assisted tryptic digestion	15 s	BSA, Myo, and Cyto C	Protein standards	BSA: 26 Myo: 80 Cyto C: 76	BSA: 38 Myo:14 Cyto C:11	-	> 5 cycles	[162]
Fe_3O_4-trypsin NPs	MW assisted tryptic digestion	15 s	Proteins	Rat liver extract	-	-	-	> 5 cycles	[162]
Fe_3O_4-trypsin NPs	MW assisted tryptic digestion	1 min	BSA	Protein standard	-	-	-	-	[163]

Nanomaterial	Type of digestion	Digestion time	Analyte	Sample	Sequence coverage (%)	Peptide matched	Peptides with missed cleavages	Reuse	Ref.
Fe_3O_4-trypsin NPs	MW assisted tryptic digestion	1 min	Proteins	Human lens tissue	-	-	-	-	[163]
commercial MNPs-trypsin	On-line tryptic digestion	1 min	Insulin chain b oxidized and β-casein	Protein standards	Casein: 45 Insulin: 100	-	-	No	[164]
Fe_3O_4@SiO_2-trypsin NPs	Tryptic digestion	16 h	BSA	Protein standard	50	-	48 %	Numerous uses during 27 days	[165]
Fe_3O_4@SiO_2-trypsin NPs	Atmospheric pressure tryptic digestion	overnight	Mixture: BSA, ovalbumin, Myo, carbonic anhydrase, and lactoglobulin	Protein standards	54	-	25 %	Numerous uses during 27 days	[165]
Fe_3O_4@SiO_2-trypsin NPs	Pressure cycling tryptic digestion	1 min	Mixture: BSA, ovalbumin, Myo, carbonic anhydrase, and lactoglobulin	Protein standards	62	-	49 %	Numerous uses during 27 days	[165]
Fe_3O_4@SiO_2-trypsin NPs	Pressure cycling tryptic digestion	5 min	Proteins	Mouse brain	-	-	-	Numerous uses during 27 days	[165]
Fe_3O_4@SiO_2-trypsin NPs	On-beads tryptic digestion	1 h	Proteins corona	Human and bovine serum	63	-	-	-	[166]
Fe_3O_4@SiO_2-trypsin NPs	Tryptic digestion	3 h	α-casein	Protein standard	-	18	6	Loss of 15 % after 4 cycles	[167]
Fe_3O_4@SiO_2-GMA-trypsin NPs	Tryptic digestion	1-2 min	BSA and IgG	Protein standards	BSA: 93	-	-	-	[168]
Fe_3O_4@SiO_2-GMA-trypsin NPs	Tryptic digestion	1-2 min	Enolase	Thermoanaerobacter tengcongensis protein extracts	-	-	-	-	[168]
Fe_3O_4@SiO_2-GMA-trypsin and Fe_3O_4@SiO_2-GMA-G-trypsin NPs	Tryptic digestion	1 min	Proteins	Yeast	-	-	-	-	[169]

Nanomaterial	Type of digestion	Digestion time	Analyte	Sample	Sequence coverage (%)	Peptide matched	Peptides with missed cleavages	Reuse	Ref.
Fe_3O_4@SiO_2-GMA-trypsin and Fe_3O_4@SiO_2-GMA-G-trypsin NPs	Tryptic digestion	1 min	Membrane proteins	Mouse liver	-	-	-	-	[169]
Fe_3O_4@PGMA-trypsin NPs	MW assisted tryptic digestion	15 s	Cyto C	Protein standard	55	6	3	12 cycles	[170]
Fe_3O_4@PGMA-trypsin NPs	Digestion at 37 ^{0}C	1 min	Cyto C	Protein standard	48	6	2	5 cycles	[170]
Fe_3O_4@polydopamine-trypsin NPs	Tryptic digestion	30 min	Cyto C, Myo, and BSA	Protein standards	Cyto C: 92 Myo: 83 BSA: 55	Cyto C: 17 Myo: 14 BSA: 36	-	5 cycles	[171]
γ-Fe_2O_3/(PS+PSMA)–trypsin nanofibers	Tryptic digestion	10 min	Enolase	Protein standard	-	-	-	> 4 cycles	[172]
Fe_3O_4@polyaniline-glutaraldehyde-protease NPs	Digestion with *Penicillium aurantiogriseum* protease	45 min	Casein	Protein standard	-	-	-	5 cycles	[173]
Fe_3O_4@PAMAM dendrimer (G2.0) - protease NPs	Digestion with *Aspergillus oryzea* protease	3 h	Casein	Protein standard	-	-	-	-	[174]
Fe_3O_4@PAMAM dendrimer (G2.0) - protease NPs	Ultrasound-assisted digestion with *Aspergillus oryzea* protease	30 min	Casein	Protein standard	-	-	-	-	[174]
NON-MAGNETIC METAL-BASED NANOMATERIALS									
AuNPs-trypsin	Tryptic digestion	~2 min	Cyto C, α- and β-casein, and β-lactoglobulin	Protein standards	Cyto C: 95 α-casein: 74 β-casein: 98 β-lactogl.: 59	Cyto C: 9 α-casein: 3 β-casein: 9 β-lactogl.: 13	-	At least 8 runs	[175]
AuNPs@PEG-trypsin	Tryptic digestion	~2 min	Cyto C, α- and β-casein, and β-lactoglobulin	Protein standards	Cyto C: 94 α-casein: 74 β-casein: 98 β-lactogl.: 75	Cyto C: 25 α-casein: 23 β-casein: 15 β-lactogl.: 21	-	At least 8 runs	[175]
AgNPs/plasma polymerized aniline -trypsin	Tryptic digestion	50 min	BSA	Protein standard	-	-	-	-	[176]
AuNPs-pepsin	Pepsin digestion	4 h	Cyto C, BSA, Myo, and monoclonal anti-HSA	Protein standards	Cyto C: 68 BSA: 20 Myo: 62	-	-	3 cycles	[177]
NANOCOMPOSITES									

Nanomaterial	Type of digestion	Digestion time	Analyte	Sample	Sequence coverage (%)	Peptide matched	Peptides with missed cleavages	Reuse	Ref.
MWCNTs/Fe_3O_4 NPs@polyaniline-trypsin	Tryptic digestion	5 min	BSA, Myo and Lyz	Protein standards	BSA:46 Myo: 81 Lyz: 63	BSA:28 Myo:13 Lyz:13	BSA:12 Myo:5 Lyz:5	5 cycles	[178]
CNTs-PAMAM dendrimer (G4.0) – trypsin	On-plate tryptic digestion	15 min	Lyz and Cyto C	Protein standards	Lyz:74 Cyto C:84	-	-	-	[179]
GO-PAMAM dendrimer (G2.0) – trypsin	On-plate tryptic digestion	15 min	Cyto C, BSA, and Myo	Protein standards	Cyto C:67 BSA:85 Myo:84	Cyto C:12 BSA:37 Myo:14	-	-	[180]
GO-PAMAM dendrimer (G2.0) – trypsin	On-plate tryptic digestion	1 h	Proteins	Human plasma	-	-	-	-	[180]
Poly(methyl methacrylate) microchip – zeolite (SiO_2) NPs-trypsin	Tryptic digestion	< 5 s	Cyto C and BSA	Protein standards	Cyto C:77 BSA:39	Cyto C:11 BSA:38	-	Yes	[181]
OTHERS									
Mesoporous SiO_2-trypsin NTs	Tryptic digestion	3 min	α-casein	Protein standard	61	15	-	-	[182]
SiO_2@cellulose-trypsin NPs	Tryptic digestion	30 min	Casein, BSA, Cyto C, and collagen	Protein standards	BSA: 88 Cyto C: 62	-	-	> 15 cycles	[183]

APTES: 3-aminopropyltriethoxysilane; **GMA:** glycidyl methacrylate; **HSA:** human serum albumin; **IgG:** human immunoglobulin G; **Lyz:** lysozyme; **MW:** microwaves; **Myo:** myoglobin; **ND:** nanodiamonds; **NIR:** near infrared; **NTA:** nitriloacetic acid; **oMWCNTs:** oxidized multi-walled carbon nanotubes; **PAMAM:** poly(amidoamine); **PGMA:** poly(glycidyl methacrylate); **PS:** polystyrene; **PSMA:** poly(styrene-co-maleic anhydride).

FIGURE CAPTIONS

Figure 1. Typical workflow for protein capture employing magnetic nanoparticles.

Figure 2. (A) HPLC-UV chromatograms corresponding to a urine sample spiked with 66.7 µg/mL lysozyme and 66.7 µg/mL Cyto C and **(B)** spiked with 66.7 µg/mL lysozyme and 133.4 µg/mL Cyto C. In chromatograms: (1) Protein mixture not treated with Fe_3O_4@molecularly imprinted polymer (MIP) nanoparticles (NPs), (2) supernatant after treating the protein mixture with Fe_3O_4@MIP NPs, and (3) solution released from Fe_3O_4@MIP NPs (Proteins release in a lower volume, improving lysozyme signal). Reproduced with permission from [60].

Figure 3. (A) Image of a third-generation carboxylate-terminated carbosilane dendrimer solution and of solutions obtained by the addition of myoglobin to the dendrimer solutions at different ratios and pH 1.8. **(B)** Profiles, obtained by SDS-PAGE, corresponding to the supernatant resulting when treating a three-protein mixture (BSA, lysozyme, and myoglobin) with different dendrimer ratios (1:0, 1:1, 1:8, and 1:20) at pH 1.8, the precipitate obtained after centrifugation of the solution with a 1:20 protein:dendrimer ratio, and the precipitate obtained when employing acetone precipitation. Reproduced with permission from [40].

Figure 4. Scheme of the metal chelation to nitriloacetic acid (NTA) and iminodiacetic acid (IDA) and the interaction established with a 6xHis-tag protein.

Figure 5. Digestion process employing **(A)** nanoparticles adsorbing proteins previous to the addition of the free enzyme or **(B)** trypsin bound nanoparticles.

Figure 6. (A) Matrix-assisted laser desorption/ionization (MALDI)-time of flight (TOF) mass spectra of cytochrome C (Cyto C) digest obtained using the magnetic enzyme nanosystem (MEN) in 30 min, **(B)** by in-solution digestion for 30 min, and **(C)** by in-solution digestion for 12 h. Reproduced with permission from [169].

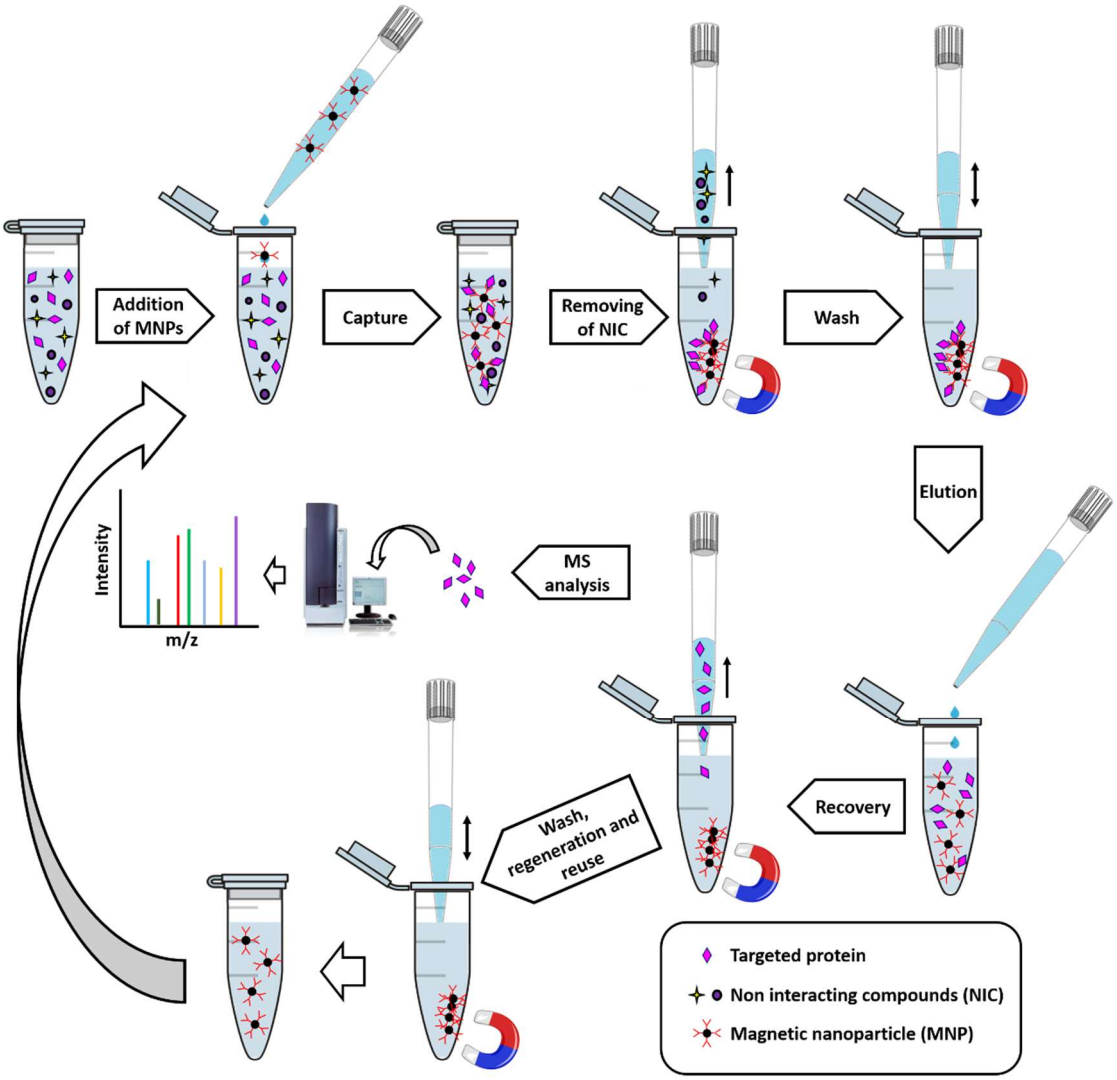

1384

1385 **Figure 1**

1386

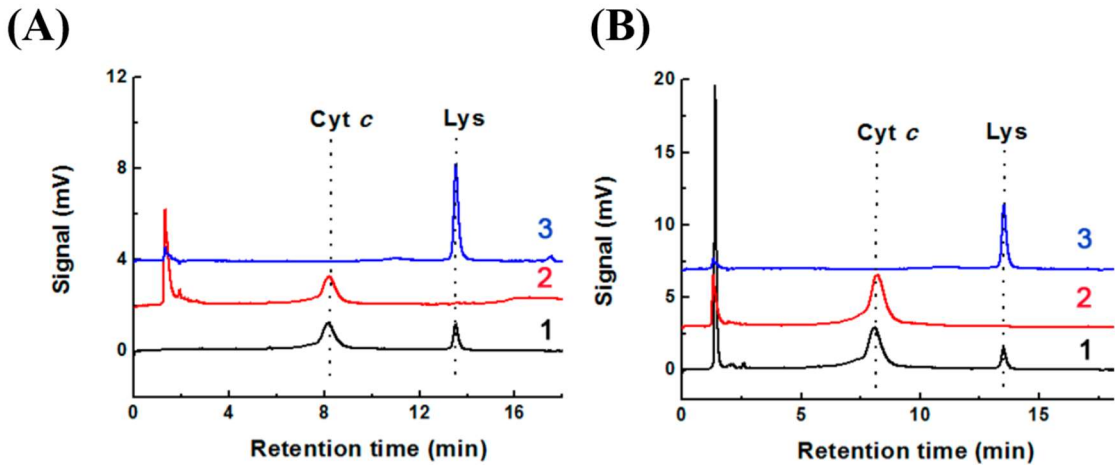

1387

1388 **Figure 2**

1389

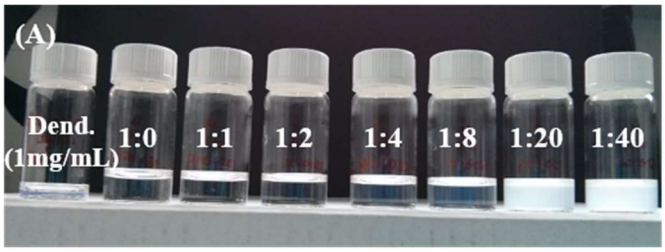

(B)

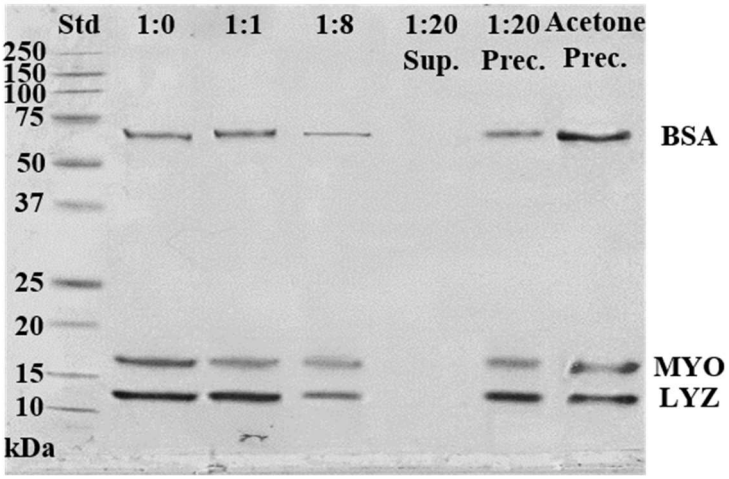

1390

1391

1392 **Figure 3**

1393

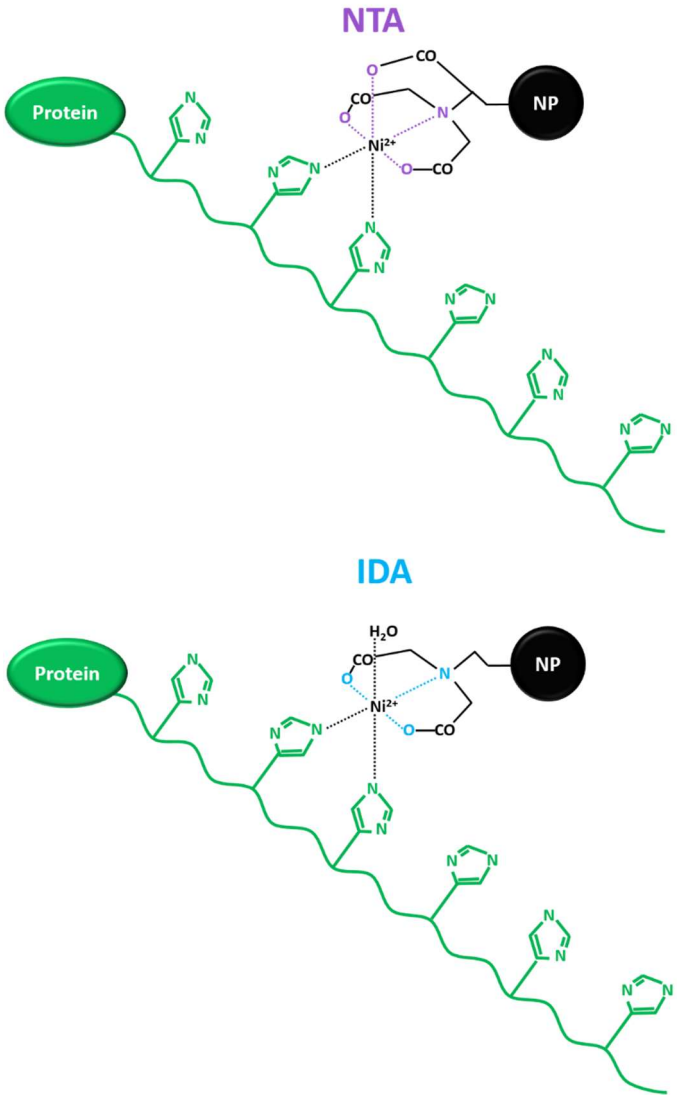
NTA
Protein
NP
CO
O
CO
O
N
Ni²⁺
N
N
O
CO
N
N
N
N
N
N
N
N
IDA
Protein
NP
H₂O
CO
O
N
Ni²⁺
N
N
O
CO
N
N
N
N
N
N
N
N

Figure 4

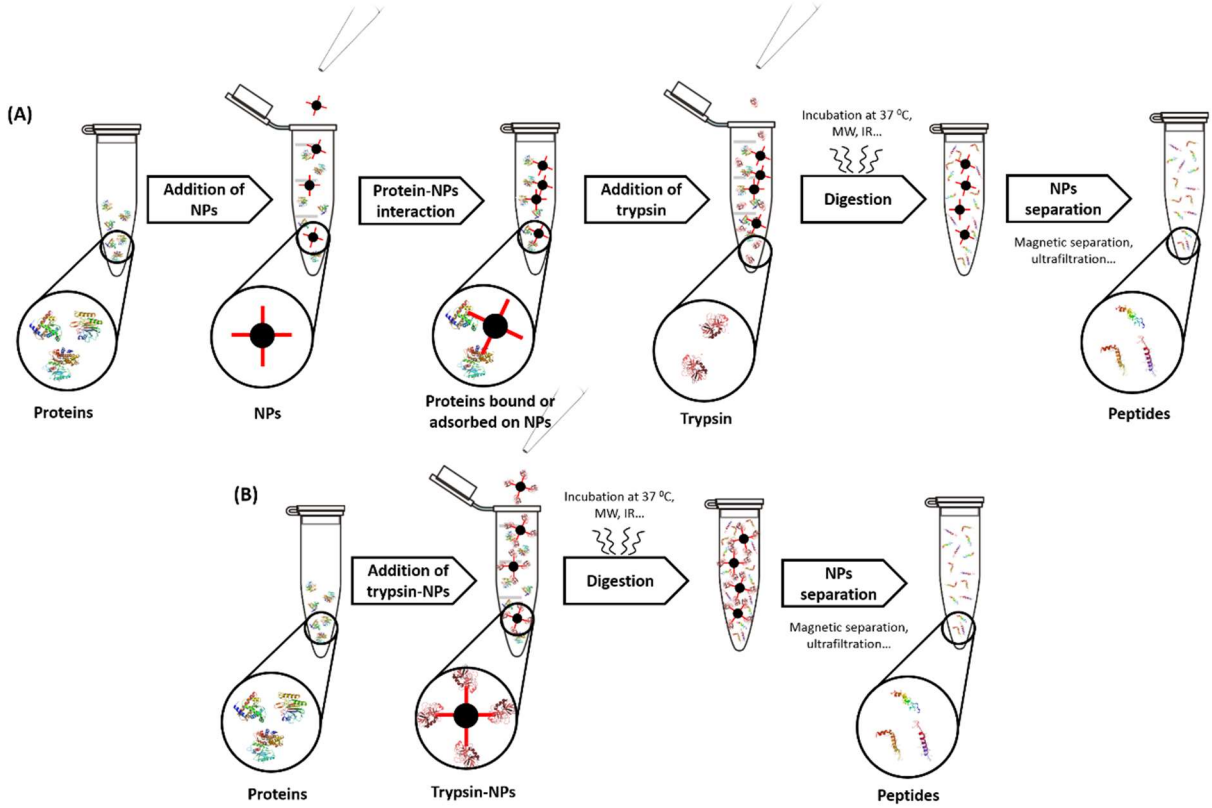

1399

1400 **Figure 5**

1401

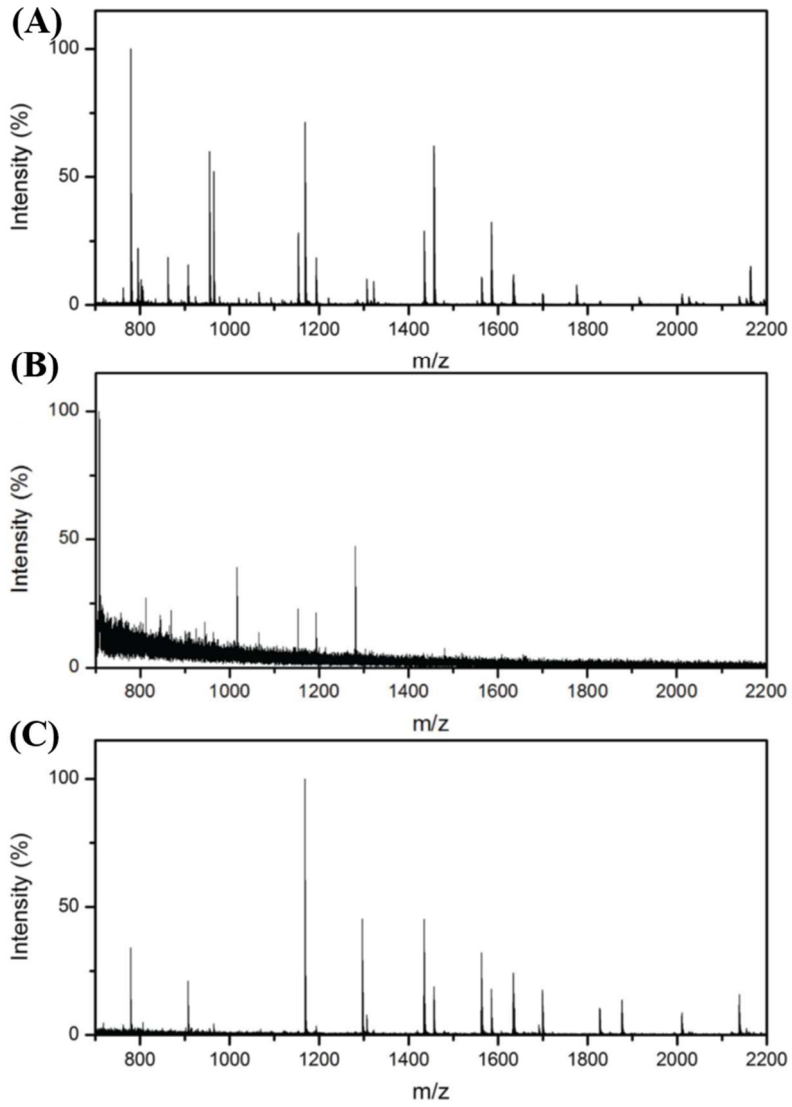

1402

1403 **Figure 6**

1404

1405

1406